Expression of Wnt Receptors in Adult Spiral Ganglion Neurons: Frizzled 9 Localization at Growth Cones of Regenerating Neurites

S. M. Shah,[a-c] Y.-J. Kang,[a-c] B. L. Christensen,[a,c], A. S. Feng,[a-c] and R. Kollmar[a-d,*]

[a]*Department of Molecular and Integrative Physiology, University of Illinois at Urbana-Champaign, Urbana, IL 61801, USA.*

[b]*Neuroscience Graduate Program, University of Illinois at Urbana-Champaign, Urbana, IL 61801, USA.*

[c]*Beckman Institute for Advanced Science and Technology, University of Illinois at Urbana-Champaign, Urbana, IL 61801, USA.*

[d]*Current address: Department of Cell Biology, SUNY Downstate Medical Center, Brooklyn, NY 11203, USA.*

[*]*Corresponding author: Department of Cell Biology, SUNY Downstate Medical Center, 450 Clarkson Ave., Box 5, Brooklyn, NY 11203, USA. Tel: x1-718-270-1014; fax: x1-718-270-3732. E-mail address: richard.kollmar@downstate.edu (R. Kollmar).*

Section Editor: Dr. Constantino Sotelo (Cellular Neuroscience)

Abbreviations

EfnB1, ephrin B1

Ephb, Eph receptor B

Fzd, frizzled homolog (Drosophila)

GEO, Gene Expression Omnibus

P10, postnatal day 10

RT-PCR, reverse transcription and polymerase chain reaction

Ryk, receptor-like tyrosine kinase

TUBB3, βIII-tubulin protein

Wnt, wingless-related MMTV integration site

Abstract

Little is known about signaling pathways, besides those of neurotrophic factors, that are operational in adult spiral ganglion neurons. In patients with sensorineural hearing loss, such pathways could eventually be targeted to stimulate and guide neurite outgrowth from the remnants of the spiral ganglion towards a cochlear implant, thereby improving the fidelity of sound transmission. To systematically identify neuronal receptors for guidance cues in the adult cochlea, we conducted a genome-wide cDNA microarray screen with two-month-old CBA/CaJ mice. A meta-analysis of our data and those from older mice in two other studies revealed the presence of neuronal transmembrane receptors that represent all four established guidance pathways—ephrin, netrin, semaphorin, and slit—in the mature cochlea as late as 15 months. In addition, we observed the expression of all known receptors for the Wnt morphogens, whose neuronal guidance function has only recently been recognized. *In situ* hybridizations located the mRNAs of the Wnt receptors frizzled 1, 4, 6, 9, and 10 specifically in adult spiral ganglion neurons. Finally, frizzled 9 protein was found in the growth cones of adult spiral ganglion neurons that were regenerating neurites in culture. We conclude from our results that adult spiral ganglion neurons are poised to respond to neurite damage, owing to the constitutive expression of a large and diverse collection of guidance receptors. Wnt signaling, in particular, emerges as a candidate pathway for guiding neurite outgrowth towards a cochlear implant after sensorineural hearing loss.

Keywords

Cell surface receptors

Cochlea

In situ hybridization

Mice

Microarray analysis

The cochlear implant is one of the most successful neural prostheses (Clark, 2003). It can initiate or restore hearing in patients with sensorineural deafness, which is commonly caused by noise, age, ototoxic drugs, or inherited mutations and is the most common sensory deficit in developed countries among humans at any age (Gates and Mills, 2005; Smith et al., 2005). With current implant designs, however, the effective number of frequency bands is inadequate for conversing in a noisy environment, grasping tonal and prosodic elements of speech, or listening to music (Shannon, 2005). A major reason for this functional deficit is the current spread over the considerable distance between the electrodes implanted in the scala tympani and their targets, the somata of the spiral ganglion neurons in Rosenthal's canal. Minimizing this distance by promoting and guiding the growth of neurites towards the electrodes could reduce the electrical interference and substantially improve the quality of hearing (Wilson et al., 2003). This would be a major improvement for the increasing number of implantees who became deaf post-lingually and are used to a higher fidelity of sound reception (Zeng, 2004).

Sensorineural hearing loss characteristically results in the rapid degeneration of the neurites between the spiral ganglion and the organ of Corti because the sensory hair cells are damaged or missing and cannot provide trophic support (Spoendlin, 1975; Gillespie and Shepherd, 2005). However, the somata and axonal projections to the brainstem can survive for many years (Nadol et al., 1989). Moreover, spontaneous, but sparse reinnervation of the organ of Corti has been observed in damaged animal cochleae *in vivo* (Lawner et al., 1997; Sugawara et al., 2005) as well as *in vitro* (Martinez-Monedero et al., 2006). Furthermore, neurites can regrow *in vitro* from the trunks of dissociated and cultured adult spiral ganglion neurons (Wei et al., 2007; reviewed in Vieira et al., 07). Together, these observations indicate that adult spiral

ganglion neurons retain the capacity to regenerate neurites and that at least some guidance cues remain in place.

Studies of embryonic and early postnatal ear development suggest three principal groups of agents that might be used therapeutically to stimulate and guide neuritogenesis in the adult cochlea: First, neurotrophic factors—ciliary neurotrophic factor, leukemia inhibitory factor, brain derived neurotrophic factor, and neurotrophin 3, as well as fibroblast growth factors—can also exert tropic effects on spiral ganglion neurites (Rubel and Fritzsch, 2002; Gillespie and Shepherd, 2005). The last three factors have indeed been reported to promote neurite regeneration in the adult cochlea (Ernfors et al., 1996; Wise et al., 2005; Miller et al., 2007; Glueckert et al., 2008). Their expression patterns, though, suggest that neurotrophic factors are unlikely to choreograph the intricate pattern of cochlear innervation by themselves (Fritzsch et al., 2005). Second, members of each of the four established guidance-factor families—ephrins, netrins, semaphorins, and slits—have been detected in the developing cochlea (Webber and Raz, 2006; Fekete and Campero, 2007); a guidance function has been demonstrated so far only for Eph receptor A4 and netrin 1 *in vitro* (Brors et al., 2003; Lee and Warchol, 2008). Third, "wingless-related MMTV integration site" (Wnt) proteins are expressed throughout ear development at least until early postnatal stages (Daudet et al., 2002; Sienknecht and Fekete, 2008). Recently, these classic morphogens have also been recognized as guidance cues throughout the nervous system (Salinas and Zou, 2008). Wnts are attractive candidates for providing guidance in a labyrinthine organ like the cochlea because of their rich combinatorial repertoire of nineteen ligands, ten "frizzled homolog (Drosophila)" *(Fzd)* receptors plus "receptor-like tyrosine kinase" *(Ryk)*, and three intracellular pathways (canonical, planar-cell polarity, and Wnt/Ca^{2+}). To date, however, no systematic studies have been undertaken to

determine which neuritogenic pathways, other than those of the neurotrophic factors, are operational in adult spiral ganglion neurons.

To identify receptors for guidance cues in the mature cochlea, we conducted a genome-wide cDNA microarray screen with modioli from adult mice. Furthermore, we investigated whether Wnt receptors are expressed in adult spiral ganglion neurons *in vivo* and are targeted to the growth cones of regenerating neurites *in vitro*. Based on our findings, we propose that manifold pathways related to neuritogenesis remain useable in the mature cochlea and that Wnt signaling could be harnessed to stimulate and guide neurite outgrowth towards an implant in a damaged adult cochlea.

Experimental Procedures

Animals

Mice, strain CBA/CaJ (The Jackson Laboratory, Bar Harbor, ME), were maintained in our own colony. All experiments were conducted in accordance with protocols approved by the University of Illinois Institutional Animal Care and Use Committee.

Microarray hybridization

Animals were sacrificed at 8 weeks of age. From each cochlea, the modiolus containing the somata of the spiral ganglion neurons was dissected as cleanly as possible within 8 min, homogenized in Trizol (Invitrogen, Carlsbad, CA), and stored at -80°C. After purifying total RNA for each animal separately, its integrity was confirmed and its amount determined by capillary electrophoresis (2100 Bioanalyzer, Agilent Technologies, Santa Clara, CA). The six RNA samples were then linearly amplified and biotinylated with an Ovation Biotin kit (NuGEN, San Carlos, CA). The yields per animal of total RNA, amplified cDNA, and biotinylated and fragmented cDNA ranged from 8 to 21 ng, 5.2 to 6.4 μg, and 3.5 to 5.1 μg, respectively. Biotinylated cDNA from each animal was hybridized to a separate Mouse Expression Set 430 2.0 array (Affymetrix, Santa Clara, CA) and imaged at the Roy J. Carver Biotechnology Center of the University of Illinois at Urbana-Champaign. Statistical analyses were conducted with R software (version 2.8.1; R Development Core Team, 2008). The original cell intensities as well as descriptions of the pre-processing with Bioconductor tools (release 2.1; Gentleman et al., 2005), the probe-set selection on the basis of hybridization signal and Gene Ontology annotation (Ashburner et al., 2000), and the meta-analysis together with the data of Someya et al. (2007; 2008) have been deposited in the public Gene Expression Omnibus database (GEO;

http://www.ncbi.nlm.nih.gov/geo/; Barrett et al., 2007) under the accession GSE12810. For genes with more than multiple probe sets on the microarray, the one with the strongest hybridization signal was taken as representative.

Half the animals used for microarray hybridization and for real-time reverse transcription and polymerase chain reaction (RT-PCR; see below) had been exposed at four weeks of age to 5-20 kHz band-limited noise at 110 dB sound pressure level. After sacrifice one month later, however, we observed at best marginal differences in chronic gene-expression levels between the noise-exposed and unexposed groups (GEO entry GSE12810 and data not shown). The data from both groups were, therefore, pooled for the analyses presented here.

Reverse transcription and polymerase chain reaction

Oligonucleotide primers for RT-PCR were taken from the RTPrimerDB (Pattyn et al., 2006) and PrimerBank (Wang and Seed, 2003) databases or designed with Primer3 software (Rozen and Skaletsky, 2000; see Table 1). Total RNA was isolated from two-month-old modioli as above, treated with DNase (Turbo DNA-free kit; Ambion), and quantitated by fluorometry. First-strand cDNA was synthesized from equal amounts of RNA at 50°C with oligo$(dT)_{18}$, RNase inhibitor (SuperaseIn; Ambion), and reverse transcriptase (Superscript III; Invitrogen). For mock cDNA synthesis, the reverse transcriptase was heat-inactivated at 90°C for 5 min beforehand, and the reaction was frozen immediately after assembly.

For qualitative assays, the amplification reactions included Taq DNA polymerase (Invitrogen), 0.2 μM of each primer (Table 1), and pooled cDNA corresponding to 1 ng/μl of RNA; after 30 cycles with an annealing temperature of 55°C, the products were analyzed by agarose-gel electrophoresis. The DNase treatment and mock cDNA synthesis were included to ensure that the PCR products were derived from mRNA and not genomic DNA, since most *Fzd*

genes lack introns. In addition, the findings were replicated independently by another experimenter with a new set of reagents in a separate building.

For real-time assays, the reactions comprised a reagent blend (iQ SYBR Green Supermix; Biorad, Hercules, CA), 0.4 μM of each primer (Table 1), and cDNA from individual mice corresponding to 0.2 ng/μl of RNA. They were denatured at 95°C for 3 min, followed by 45 cycles of denaturation at 95°C, annealing at 55°C, and extension at 72°C for 30 s each (iCycler iQ; Biorad). The fluorescence signal was specific, since neither primer dimers nor products of the wrong size were detected on melting curves and agarose gels. A common threshold signal was chosen manually in the linear amplification range of all samples by inspecting the log-transformed fluorescence plotted against the cycle number (iCycler iQ Optical System Software, Version 3.0a; BioRad).

In situ hybridization

Partial mouse *Fzd* and *Ryk* cDNAs were amplified in RT-PCRs with the primers shown in Table 1 and cloned into the vector pBluescript II SK (+) (Stratagene, La Jolla, CA). Digoxigenin-labeled riboprobes were synthesized from these templates as described (Kang et al., 2008); their concentration and integrity were confirmed by dot blotting and by gel electrophoresis and antibody detection after membrane transfer. Two-month-old cochleae were fixed by immersion in 4% wt/vol paraformaldehyde in phosphate-buffered saline at 4°C overnight, decalcified in 0.5 M EDTA (pH 7.0) at 4°C for three days, and embedded in paraffin (Paraplast Plus; SPI Supplies, West Chester, PA). Longitudinal 6 μm-thick sections were mounted on positively-charged slides (Superfrost Plus; Fisher Scientific, Pittsburgh, PA) and hybridized to detect mRNAs as described (Acloque et al., 2008). Some sections were stained with hematoxylin and eosin instead. Tiled images were stitched together with Axiovision software (release 4.5; Carl

Zeiss, Thornwood, NY). Contrast was adjusted to match the dynamic range of the digital images with Photoshop software (version 8.0; Adobe, San Jose, CA).

Immunofluorescence microscopy

Adult spiral ganglion neurons were cultured in chambered glass slides (Lab-Tek; Nalge Nunc, Rochester, NY) and labeled for immunofluorescence detection with the nuclear stain 0.3 μM 4',6-diamidino-2-phenylindole (DAPI; Molecular Probes, Eugene, OR), 2 μg/ml Alexa-488-conjugated monoclonal mouse antibody against the neuronal marker βIII-tubulin (TUBB3; Covance, Princeton, NJ), 5 μg/ml affinity-purified polyclonal rabbit antibodies against human and mouse FZD9 protein (ab13000; Abcam, Cambridge, MA), and 7.5 μg/ml rhodamine-conjugated donkey anti-rabbit-IgG antibodies (Jackson ImmunoResearch Laboratories, West Grove, PA) as described (Vieira et al., 2007). As a negative control, the antibodies against FZD9 were omitted or replaced with purified normal rabbit IgG (Jackson) at the same concentration. The digital images were processed as above for *in situ* hybridization.

Results

Manifold neuronal receptors expressed in the adult cochlea

To determine which potential guidance receptors were present in the adult cochlea, we conducted a microarray hybridization screen with dissected modioli from six 8-week-old CBA/CaJ mice. First, we sought to establish a rational criterion to discern expressed genes. The probability density plot of the hybridization signals for all 45,101 probe-sets and all six mice suggested two slightly overlapping probe-set distributions (Fig. 1): The first was narrow and almost symmetrical, with a center near the low end of the range; the second was broad and skewed, with a long tail towards the high end of the range. Because the former represented most likely probe sets with background hybridization signals, we chose the crossover point of the two distribution functions, the 44th percentile, as the cutoff for true expression in our further analyses.

Next, we looked for evidence of robust expression of potential guidance receptors. For increased statistical power, we focused our analysis on 1,369 probe sets representing 738 genes with a Gene Ontology annotation as neuronal transmembrane receptors. In addition, we combined our modiolus data with those from the untreated control mice in two studies that had used the same microarray platform to measure differential gene expression in older cochleae (Someya et al., 2007; Someya et al., 2008). The Pearson coefficient for all hybridization signals between the three data series ranged from 0.55 to 0.87, indicating that there was a significant correlation ($P \leq 5 \cdot 10^{-4}$) despite the differences in age, strain, and sample preparation and that a meta-analysis was legitimate. In the pooled data from all 17 mice, 339 of the 1,369 probe sets for neuronal transmembrane receptors representing 242 unique genes exhibited a mean hybridization signal that was significantly higher than the 44th-percentile cutoff ($P < 0.05$ after Bonferroni correction in one-sided *t* tests); another 300 probe sets, including 177 more unique genes,

exhibited a mean hybridization signal that was higher than, but not significantly different from the cutoff (Supplemental Table 1). Similar results were obtained when our hybridization data were analyzed alone. All four established guidance-factor pathways were represented among the expressed genes (Table 2). Likewise, all eleven Wnt receptors were present—*Fzd1* to *Fzd10* and *Ryk*—as well as two co-receptors. In addition, most receptors for neurotrophic factors were detected (see Supplemental Table 1). We concluded from the results of our exploratory microarray screen and meta-analysis that an ample repertoire of neuronal signaling pathways is available in the adult cochlea.

Five Fzd genes expressed in adult spiral ganglion neurons

To confirm and extend our microarray findings, we concentrated on the Wnt pathway, whose involvement in cochlear neuritogenesis had not been investigated previously. First, we qualitatively confirmed the presence of the *Fzd1* to *Fzd10* and *Ryk* mRNAs by using the RT-PCR as an independent method. Products of the expected size were amplified for all eleven genes from a template of modiolar RNA subjected to cDNA synthesis (Fig. 2). This result was consistent with our observation of microarray signals above the cutoff for all eleven Wnt receptors.

Next, we conducted *in situ* hybridizations to determine which, if any, of the *Fzd* and *Ryk* genes were expressed in spiral ganglion neurons. On longitudinal sections of cochleae from 6-to-8-week-old mice, antisense riboprobes for *Fzd1, -4, -6, -9,* and *-10* specifically labeled the somata of spiral ganglion neurons in Rosenthal's canal (Fig. 3). Intriguingly, the labeling in the cochlea decreased from the apical to the basal turns for *Fzd1,-4,* and *-10,* suggesting a gradient of expression along the cochlea's tonotopic map. The antisense *Fzd6* probe also bound to most cells in the saccular macula and to neurons in Scarpa's ganglion next to the cochlea's base (Fig. 4).

Finally, we quantified the abundance of Wnt receptor mRNAs in the modiolus by performing real-time RT-PCRs. Some of the *Fzd* genes that had not exhibited specific labeling of spiral ganglion neurons (Fig. 3) were omitted from the experiment. The mean mRNA levels across 12 nine-week-old mice, as measured individually by real-time RT-PCR, correlated strongly with those measured before by microarray hybridization (Fig. 5). The results of these gene-specific experiments lend strong support to our genome-wide assessment of guidance-receptor expression in the cochlea. Furthermore, they demonstrate that adult spiral ganglion express up to five different Wnt receptors at a robust level.

FZD9 protein targeted to growth cones of regenerating spiral ganglion neurons

Finally, we employed immunofluorescence microscopy to examine whether spiral ganglion neurons sport Wnt receptors at sites of neurite regrowth. We used antibodies against FZD9, whose cognate mRNA had been detected in all of our microarray, RT-PCR, and *in situ* hybridization analyses (see above). Spiral ganglion neurons from adult mice were dissociated, and their trunks allowed to regrow neurites in serum-free culture as an *in vitro* model of regeneration. Immunofluorescence microscopy located FZD9 specifically in all neurons, in particular at the growth cones, regardless of the number and the length of neurites (Fig. 6A-C and G-I). Qualitatively, the FZD9 fluorescence appeared to be stronger in spindle-shaped "simple" growth cones than in branched "complex" growth cones. This result was consistent with the detection of *Fzd9* mRNA from apex to base and demonstrated that FZD9 occurs in the right place to modulate and guide neurite regeneration in adult spiral ganglion neurons.

Discussion

Our results show that a large and diverse collection of neuronal transmembrane receptors representing all four established guidance pathways—ephrin, netrin, semaphorin, and slit—is present in the adult mouse cochlea. We also observed expression of all Wnt receptors and located the mRNAs of *Fzd1, -4, -6, -9,* and *-10* specifically in adult spiral ganglion neurons. Finally, we detected FZD9 protein in the growth cones of adult spiral ganglion neurons that were regenerating neurites in culture.

The detection of dozens of guidance receptors in the adult cochlea as late as 15 months may come as a surprise. After all, the innervation of the murine organ of Corti is complete by the time hearing commences on postnatal day 10 (P10; Huang et al., 2007). Previous studies of global gene expression in the adult cochlea have published in general only small excerpts of their primary data and not focused on neuronal receptors as a group. We closed this gap by combining our own data from the modioli of two-month-old mice with two data sets in the public GEO database from the cochleae of four- to fifteen-month-old mice that had been collected on the same microarray platform (Someya et al., 2007; Someya et al., 2008). The hybridization signals for neuronal receptors in these three independent data sets were in close agreement. Furthermore, the signals corresponded well with our RT-PCR results for all eleven Wnt receptors and five other test genes, which covered a wide range of mRNA levels. In addition, the results of our meta-analysis were largely consistent with microarray data from one-month-old CBA/CaJ mice by Chen and Corey (2002; see Table 2). Finally, expression of assorted guidance receptors in the adult cochlea or specifically in spiral ganglion neurons has been demonstrated in several studies that employed RT-PCR or immunocytochemistry (see Table 2). Taken together, these

concordances indicate that our microarray results faithfully represent the expression of neuronal transmembrane receptors in the adult cochlea.

The expression of specific *Fzd* genes in adult spiral ganglion neurons is a continuation of the pattern reported previously for the embryonic ganglion and the early postnatal cochlea. In the developing ear, the Wnt pathway functions in otic induction (Ohyama et al., 2007), axis and boundary specification (Bok et al., 2007), the regulation of planar cell polarity, particularly in hair cells (Montcouquiol et al., 2006a), and vascularization, with the atypical norrin ligand (Xu et al., 2004). Accordingly, numerous *Fzd* genes have been found to be expressed throughout the embryonic and early postnatal ear (Wang et al., 2001; Stevens et al., 2003; Visel et al., 2004; Xu et al., 2004; Montcouquiol et al., 2006b; Wang et al., 2006; Sajan et al., 2007). The latest stages investigated have been P14 in the rat, with *Fzd1* to *-4, -6,* and *-9* detected in the cochlea by RT-PCR (Daudet et al., 2002). The auditory ganglion is mentioned only by Sienknecht and Fekete in their thorough study of the chicken's developing cochlear duct (2008): strong expression for *Fzd1* and *-9;* moderate for *Fzd2,-4, -7,* and *-8;* and none for *Fzd10*. Allowing for inter-species differences, the latter two reports agree well with our findings of *Fzd1, -4, -6, -9,* and weak *-10* expression in spiral ganglion neurons of the adult mouse.

What roles might the neuronal receptors play in the adult cochlea? For most of the classic guidance receptors, the cellular location has not been ascertained, and their cognate pathways participate in a wide range of developmental and homeostatic processes outside the nervous system (Hinck, 2004). Nevertheless, at least some of the ephrin, netrin, semaphorin, and slit receptors may provide guidance to spiral ganglion neurons, as evidenced by the responsiveness of cultured neurons from mice at P28 to P35 to netrin 1 (Lee and Warchol, 2008).

For *Fzd1, -4, -6, -9,* and *-10,* the selective expression in adult spiral ganglion neurons shown here also suggests roles related to neuritogenesis and synapse formation, as documented elsewhere in the nervous system (Salinas and Zou, 2008), rather than to the classic morphogenetic processes during ear development. (We cannot speak to the other Wnt receptors, as we could not locate them in our *in situ* hybridizations.) Our detection of FZD9 protein in the growth cones of regenerating neurites *in vitro* is consistent with this hypothesis, but its presence in adult growth cones *in vivo* remains to be to demonstrated. Further support comes from the complementary localization of the Wnts themselves, although systematic studies have been conducted only at embryonic and postnatal stages of development: In the chicken embryo, *Wnt4, -5a, -5b, -7a, -7b, -9a,* and *-11,* as well as the Wnt inhibitors "secreted frizzled-related protein" 2 and 3, are expressed mostly in non-sensory domains that extend along the cochlea's long axis (Sienknecht and Fekete, 2008). In the rat cochlea at P14 and P21, *Wnt4, -5b,* and *-7a* expression has been located in domains that surround the neurites and somata; *Wnt7a* mRNA has also been located in spiral ganglion neurons and outer hair cells (Daudet et al., 2002). Chen and Corey in the analysis of their microarray data have pointed out a prevalence of *Wnt4, -5a, -5b,* and *-7b* expression in mouse cochleae at P32 (2002), and our preliminary RT-PCR experiments have detected a similar set of *Wnt* mRNAs in two-month-old animals (S.M. Shah, unpublished observations). Since Wnts do not seem to be secreted from inner hair cells, the targets of the spiral ganglion neurons, their presumptive guidance role may be mostly repulsive, keeping neurites from straying from their path to the organ of Corti.

The Wnts in the cochlea most likely join forces with other signaling factors, as they do elsewhere in the nervous system; for example, WNT3 regulates the arborization of neurotrophin-3-responsive sensory neurons in the spinal cord (Krylova et al., 2002), and parallel gradients of

WNT3/RYK and EFNB1/EPHB ligand/receptor pairs control the topographic mapping of retinotectal projections (Schmitt et al., 2006). The plenitude of possible Wnt ligand-receptor combinations also leaves room for other roles, such as guidance of the axonal projections from the spiral ganglion to the brainstem (Rubel and Fritzsch, 2002) and control of neuronal survival and death (Ille and Sommer, 2005). We therefore propose that stable complements of both Wnt and frizzled proteins are present in the cochlea from embryonic to adult stages and provide guidance cues to the spiral ganglion neurons for neurite outgrowth, maintenance, and regeneration in conjunction with other neurotrophic and neurotropic signals.

Our finding of a large number of known and potential guidance receptors in the adult cochlea suggests that its neurons are not static and are poised to respond to damage. Functional experiments *in vitro* and *in vivo* will show whether the established guidance pathways as well as Wnt signaling can be harnessed to augment neurotrophic treatments and promote and guide the regeneration of damaged neurites after sensorineural hearing loss.

Acknowledgements

We thank Dr. Steven Clough for the use of his Agilent Bioanalyzer, Dr. Mark Band for advice on microarray hybridizations, Dr. Shinichi Someya and colleagues for making their microarray data publicly available, Drs. Zheng-Yi Chen and David Corey for sharing their microarray data, Dr. Lori Raetzman for advice on and Mr. Chirag Patel for assistance with *in situ* hybridizations, and Ms. Amy Stevenson for comments on the manuscript. This work was supported by training grant T32 DC006612 from the National Institute on Deafness and Other Communication Disorders and a medical student training grant from the American Otological Society to S.M.S., by grants from the Campus Research Board and the Mary Jane Neer Fund at the University of Illinois to A.S.F., and by University of Illinois start-up funds and a research award from the National Organization for Hearing Research to R.K.

References

Acloque H, Wilkinson DG, Nieto MA (2008) In situ hybridization analysis of chick embryos in whole-mount and tissue sections. Methods Cell Biol 87:169-185.

Ashburner M, Ball CA, Blake JA, Botstein D, Butler H, Cherry JM, Davis AP, Dolinski K, Dwight SS, Eppig JT, Harris MA, Hill DP, Issel-Tarver L, Kasarskis A, Lewis S, Matese JC, Richardson JE, Ringwald M, Rubin GM, Sherlock G (2000) Gene ontology: tool for the unification of biology. The Gene Ontology Consortium. Nat Genet 25:25-29.

Barrett T, Troup DB, Wilhite SE, Ledoux P, Rudnev D, Evangelista C, Kim IF, Soboleva A, Tomashevsky M, Edgar R (2007) NCBI GEO: mining tens of millions of expression profiles--database and tools update. Nucleic Acids Res 35:D760-5.

Bianchi LM, Dinsio K, Davoli K, Gale NW (2002) Lac z Histochemistry and immunohistochemistry reveal ephrin-B ligand expression in the inner ear. J Histochem Cytochem 50:1641-1645.

Bianchi LM, Gale NW (1998) Distribution of Eph-related molecules in the developing and mature cochlea. Hear Res 117:161-172.

Bianchi LM, Liu H (1999) Comparison of ephrin-A ligand and EphA receptor distribution in the developing inner ear. Anat Rec 254:127-134.

Bok J, Chang W, Wu DK (2007) Patterning and morphogenesis of the vertebrate inner ear. Int J Dev Biol 51:521-533.

Brors D, Bodmer D, Pak K, Aletsee C, Schafers M, Dazert S, Ryan AF (2003) EphA4 provides repulsive signals to developing cochlear ganglion neurites mediated through ephrin-B2 and -B3. J Comp Neurol 462:90-100.

Chen ZY, Corey DP (2002) An inner ear gene expression database. J Assoc Res Otolaryngol 3:140-148.

Clark G (2003) Cochlear Implants: Fundamentals and Applications. New York: Springer.

Daudet N, Ripoll C, Moles JP, Rebillard G (2002) Expression of members of Wnt and Frizzled gene families in the postnatal rat cochlea. Brain Res Mol Brain Res 105:98-107.

Ernfors P, Duan ML, ElShamy WM, Canlon B (1996) Protection of auditory neurons from aminoglycoside toxicity by neurotrophin-3. Nat Med 2:463-467.

Fekete DM, Campero AM (2007) Axon guidance in the inner ear. Int J Dev Biol 51:549-556.

Fritzsch B, Pauley S, Matei V, Katz DM, Xiang M, Tessarollo L (2005) Mutant mice reveal the molecular and cellular basis for specific sensory connections to inner ear epithelia and primary nuclei of the brain. Hear Res 206:52-63.

Gates GA, Mills JH (2005) Presbycusis. Lancet 366:1111-1120.

Gentleman R, Carey V, Huber W, Irizarry R, Dudoit S (2005) Bioinformatics and Computational Biology Solutions Using R and Bioconductor. New York: Springer.

Gillespie LN, Shepherd RK (2005) Clinical application of neurotrophic factors: the potential for primary auditory neuron protection. Eur J Neurosci 22:2123-2133.

Glueckert R, Bitsche M, Miller JM, Zhu Y, Prieskorn DM, Altschuler RA, Schrott-Fischer A (2008) Deafferentation-associated changes in afferent and efferent processes in the guinea pig cochlea and afferent regeneration with chronic intrascalar brain-derived neurotrophic factor and acidic fibroblast growth factor. J Comp Neurol 507:1602-1621.

Hinck L (2004) The versatile roles of "axon guidance" cues in tissue morphogenesis. Dev Cell 7:783-793.

Howard MA, Rodenas-Ruano A, Henkemeyer M, Martin GK, Lonsbury-Martin BL, Liebl DJ (2003) Eph receptor deficiencies lead to altered cochlear function. Hear Res 178:118-130.

Huang LC, Thorne PR, Housley GD, Montgomery JM (2007) Spatiotemporal definition of neurite outgrowth, refinement and retraction in the developing mouse cochlea. Development 134:2925-2933.

Ille F, Sommer L (2005) Wnt signaling: multiple functions in neural development. Cell Mol Life Sci 62:1100-1108.

Kang YJ, Stevenson AK, Yau PM, Kollmar R (2008) Sparc protein is required for normal growth of zebrafish otoliths. J Assoc Res Otolaryngol 9:436-451.

Krylova O, Herreros J, Cleverley KE, Ehler E, Henriquez JP, Hughes SM, Salinas PC (2002) WNT-3, expressed by motoneurons, regulates terminal arborization of neurotrophin-3-responsive spinal sensory neurons. Neuron 35:1043-1056.

Lawner BE, Harding GW, Bohne BA (1997) Time course of nerve-fiber regeneration in the noise-damaged mammalian cochlea. Int J Dev Neurosci 15:601-617.

Lee KH, Warchol ME (2008) Promotion of neurite outgrowth and axon guidance in spiral ganglion cells by netrin-1. Arch Otolaryngol Head Neck Surg 134:146-151.

Martinez-Monedero R, Corrales CE, Cuajungco MP, Heller S, Edge AS (2006) Reinnervation of hair cells by auditory neurons after selective removal of spiral ganglion neurons. J Neurobiol 66:319-331.

Miller JM, Le Prell CG, Prieskorn DM, Wys NL, Altschuler RA (2007) Delayed neurotrophin treatment following deafness rescues spiral ganglion cells from death and promotes regrowth of auditory nerve peripheral processes: Effects of brain-derived neurotrophic factor and fibroblast growth factor. J Neurosci Res 85:1959-1969.

Montcouquiol M, Crenshaw EB, Kelley MW (2006a) Noncanonical Wnt signaling and neural polarity. Annu Rev Neurosci 29:363-386.

Montcouquiol M, Sans N, Huss D, Kach J, Dickman JD, Forge A, Rachel RA, Copeland NG, Jenkins NA, Bogani D, Murdoch J, Warchol ME, Wenthold RJ, Kelley MW (2006b) Asymmetric localization of Vangl2 and Fz3 indicate novel mechanisms for planar cell polarity in mammals. J Neurosci 26:5265-5275.

Nadol JB,Jr, Young YS, Glynn RJ (1989) Survival of spiral ganglion cells in profound sensorineural hearing loss: implications for cochlear implantation. Ann Otol Rhinol Laryngol 98:411-416.

Ohyama T, Groves AK, Martin K (2007) The first steps towards hearing: mechanisms of otic placode induction. Int J Dev Biol 51:463-472.

Pattyn F, Robbrecht P, De Paepe A, Speleman F, Vandesompele J (2006) RTPrimerDB: the real-time PCR primer and probe database, major update 2006. Nucleic Acids Res 34:D684-8.

R Development Core Team (2008) R: A Language and Environment for Statistical Computing. Vienna, Austria: R Foundation for Statistical Computing.

Rozen S, Skaletsky H (2000) Primer3 on the WWW for general users and for biologist programmers. Methods Mol Biol 132:365-386.

Rubel EW, Fritzsch B (2002) Auditory system development: primary auditory neurons and their targets. Annu Rev Neurosci 25:51-101.

Sajan SA, Warchol ME, Lovett M (2007) Toward a systems biology of mouse inner ear organogenesis: gene expression pathways, patterns and network analysis. Genetics 177:631-653.

Salinas PC, Zou Y (2008) Wnt signaling in neural circuit assembly. Annu Rev Neurosci 31:339-358.

Schmitt AM, Shi J, Wolf AM, Lu CC, King LA, Zou Y (2006) Wnt-Ryk signalling mediates medial-lateral retinotectal topographic mapping. Nature 439:31-37.

Shannon RV (2005) Speech and music have different requirements for spectral resolution. Int Rev Neurobiol 70:121-134.

Sienknecht UJ, Fekete DM (2008) Comprehensive Wnt-related gene expression during cochlear duct development in chicken. J Comp Neurol 510:378-395.

Smith RJ, Bale JF,Jr, White KR (2005) Sensorineural hearing loss in children. Lancet 365:879-890.

Someya S, Yamasoba T, Kujoth GC, Pugh TD, Weindruch R, Tanokura M, Prolla TA (2008) The role of mtDNA mutations in the pathogenesis of age-related hearing loss in mice carrying a mutator DNA polymerase gamma. Neurobiol Aging 29:1080-1092.

Someya S, Yamasoba T, Weindruch R, Prolla TA, Tanokura M (2007) Caloric restriction suppresses apoptotic cell death in the mammalian cochlea and leads to prevention of presbycusis. Neurobiol Aging 28:1613-1622.

Spoendlin H (1975) Retrograde degeneration of the cochlear nerve. Acta Otolaryngol 79:266-275.

Stevens CB, Davies AL, Battista S, Lewis JH, Fekete DM (2003) Forced activation of Wnt signaling alters morphogenesis and sensory organ identity in the chicken inner ear. Dev Biol 261:149-164.

Sugawara M, Corfas G, Liberman MC (2005) Influence of supporting cells on neuronal degeneration after hair cell loss. J Assoc Res Otolaryngol 6:136-147.

Vieira M, Christensen BL, Wheeler BC, Feng AS, Kollmar R (2007) Survival and stimulation of neurite outgrowth in a serum-free culture of spiral ganglion neurons from adult mice. Hear Res 230:17-23.

Visel A, Thaller C, Eichele G (2004) GenePaint.org: an atlas of gene expression patterns in the mouse embryo. Nucleic Acids Res 32:D552-6.

Wang X, Seed B (2003) A PCR primer bank for quantitative gene expression analysis. Nucleic Acids Res 31:e154.

Wang Y, Guo N, Nathans J (2006) The role of Frizzled3 and Frizzled6 in neural tube closure and in the planar polarity of inner-ear sensory hair cells. J Neurosci 26:2147-2156.

Wang Y, Huso D, Cahill H, Ryugo D, Nathans J (2001) Progressive cerebellar, auditory, and esophageal dysfunction caused by targeted disruption of the frizzled-4 gene. J Neurosci 21:4761-4771.

Webber A, Raz Y (2006) Axon guidance cues in auditory development. Anat Rec A Discov Mol Cell Evol Biol 288:390-396.

Wei D, Jin Z, Järlebark L, Scarfone E, Ulfendahl M (2007) Survival, synaptogenesis, and regeneration of adult mouse spiral ganglion neurons in vitro. Dev Neurobiol 67:108-122.

Wilson BS, Lawson DT, Muller JM, Tyler RS, Kiefer J (2003) Cochlear implants: some likely next steps. Annu Rev Biomed Eng 5:207-249.

Wise AK, Richardson R, Hardman J, Clark G, O'leary S (2005) Resprouting and survival of guinea pig cochlear neurons in response to the administration of the neurotrophins brain-derived neurotrophic factor and neurotrophin-3. J Comp Neurol 487:147-165.

Xu Q, Wang Y, Dabdoub A, Smallwood PM, Williams J, Woods C, Kelley MW, Jiang L, Tasman W, Zhang K, Nathans J (2004) Vascular development in the retina and inner ear: control by Norrin and Frizzled-4, a high-affinity ligand-receptor pair. Cell 116:883-895.

Zeng FG (2004) Trends in cochlear implants. Trends Amplif 8:1-34.

Figure Legends

Fig. 1. Establishing a cutoff criterion for true expression versus background. Density distribution of the mean $\log_2$-transformed hybridization signals for all six mice (GEO accession GSE12810). Gray histogram, all 45,105 probe sets on the mouse 430 2.0 microarray; white histogram, the 1,369 probe sets annotated as neuronal transmembrane receptors, with fivefold-magnified ordinate. Solid lines, beta distributions $f(x'; \alpha, \beta)$ fitted to the gray histogram with $x' = (x - \mathit{offset}) / \mathit{scale\ factor}$. Arrow, the crossover of the fitted lines at a hybridization signal of $2^{4.25}$ corresponding to the 44th-percentile cutoff.

Fig. 2. Expression of all Wnt receptors in the modiolus of adult mice. (Top) The mRNAs of *Fzd1* to *Fzd10* and *Ryk* were detected in qualitative RT-PCRs with a cDNA template derived from two-month-old mice (see Table 1 for expected product sizes). (Bottom) No products were amplified from a mock cDNA template synthesized after heat-inactivating the reverse transcriptase. Marker sizes in base pairs indicated on the right.

Fig. 3. Selective expression of Wnt receptors in adult spiral ganglion neurons. *In situ* hybridizations of antisense riboprobes for the indicated mRNAs to longitudinal paraffin sections of cochleae from two-month old mice, with the apex at the top. Arrows point at the cross-sections of the spiral ganglion inside Rosenthal's canal; note that some cross sections lack the brown or purple hybridization signal. The smaller panels at the bottom-left and -right of each triad show details from the apical- and basal-most cross sections, respectively, as indicated for the sample stained with hematoxylin and eosin (H&E). Antisense probes for the remaining six Wnt receptors did not exhibit specific labeling, nor did any of the sense probes (data not shown).

Mod, modiolus; ScT, scala tympani; arrowheads, location of the organ of Corti with hair cells; scale bar, 300 μm for the large and 50 μm for the small panels.

Fig. 4. Expression of *Fzd6* in the adult vestibular periphery. *In situ* hybridizations of antisense riboprobes for the indicated *Fzd* mRNAs to paraffin sections from two-month old mice. Top two panels, cross-sections of the saccular sensory macula; bottom two panels, Scarpa's ganglion of the vestibular nerve. No labeling was observed for the other Wnt receptors, as exemplified for *Fzd9* and *-10,* or with sense probes. Scale bar, 40 μm for the top and 50 μm for the bottom panels.

Fig. 5. Correlation of microarray and real-time RT-PCR analyses of Wnt-receptor expression within the cochlea. The hybridization signals are from the meta-analysis of our microarray data and those of Someya and colleagues (Table 2 and Supplement Table 1). The RT-PCR threshold cycles are the means from the modioli of twelve separate, nine-week-old animals. The Pearson's coefficient for the fitted straight line equaled -0.84, indicating a significant correlation *($P < 0.001$)*. Error bars, standard deviations; gene symbols, see Table 1.

Fig. 6. FZD9 protein localized to growth cones of regenerating adult spiral ganglion neurons in primary culture. (A/D/G/J) Differential interference contrast (DIC); (B/E/H/K) three-channel epifluorescence with nuclei colored in blue, the neuronal marker βIII-tubulin in green (TUBB3), and FZD9 in red; (C/F/I/L) red-channel fluorescence alone. Only weak background labeling was observed in non-neuronal cells, or when the FZD9 antibodies were omitted (D-F) or replaced by normal rabbit IgG (J-L). Arrowheads, "simple" growth cones; arrows, "complex" growth cones; scalebar in F for panels A-F, 50 μm; scalebar in L for panels

G-I and J-L, 17.5 and 30 μm, respectively. The samples in A-F were processed and imaged under identical conditions, as were those in G-L.

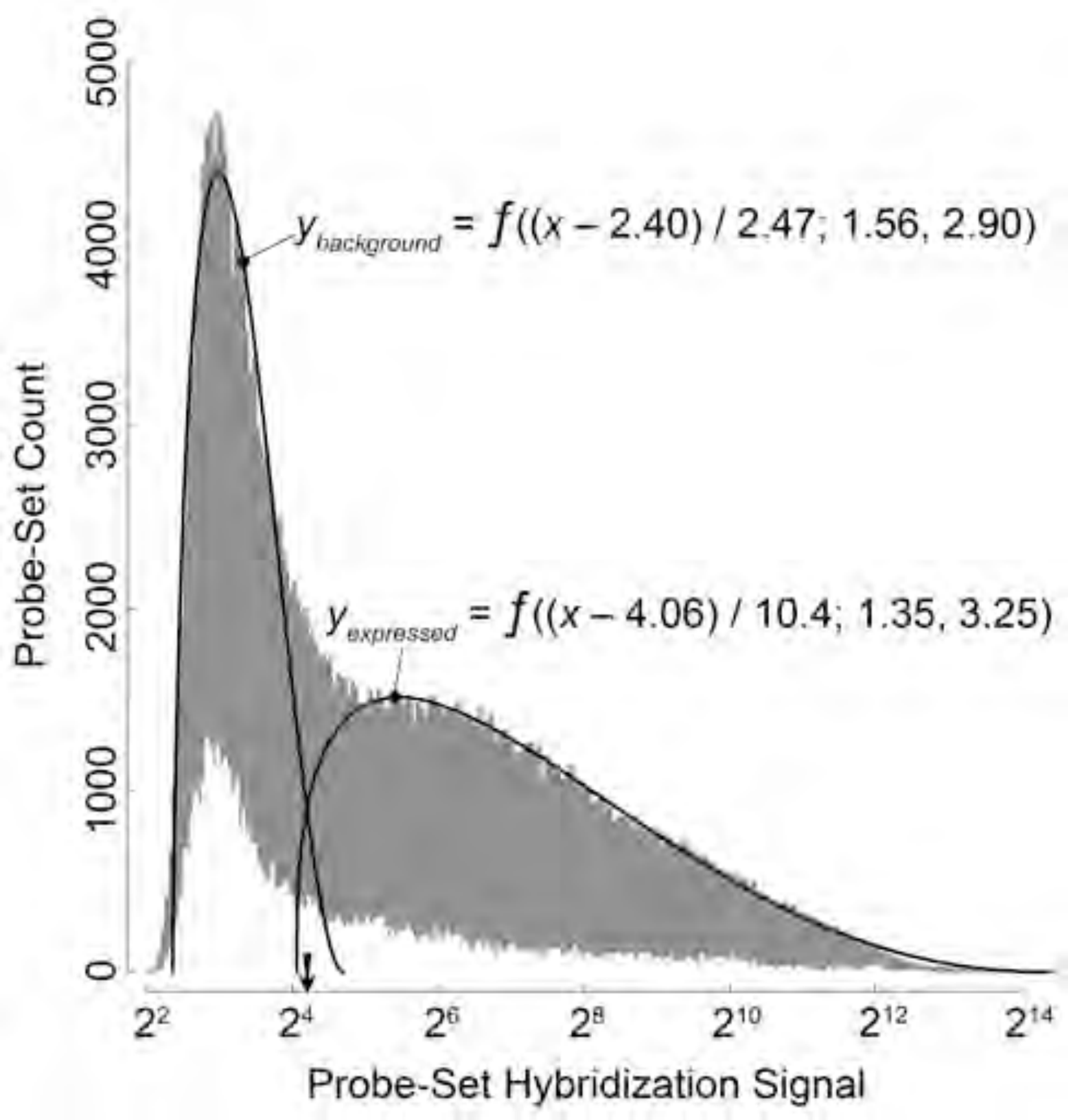
Probe-Set Count
0
1000
2000
3000
4000
5000
$y_{background} = f((x - 2.40) / 2.47; 1.56, 2.90)$
$y_{expressed} = f((x - 4.06) / 10.4; 1.35, 3.25)$
2^2
2^4
2^6
2^8
2^{10}
2^{12}
2^{14}
Probe-Set Hybridization Signal

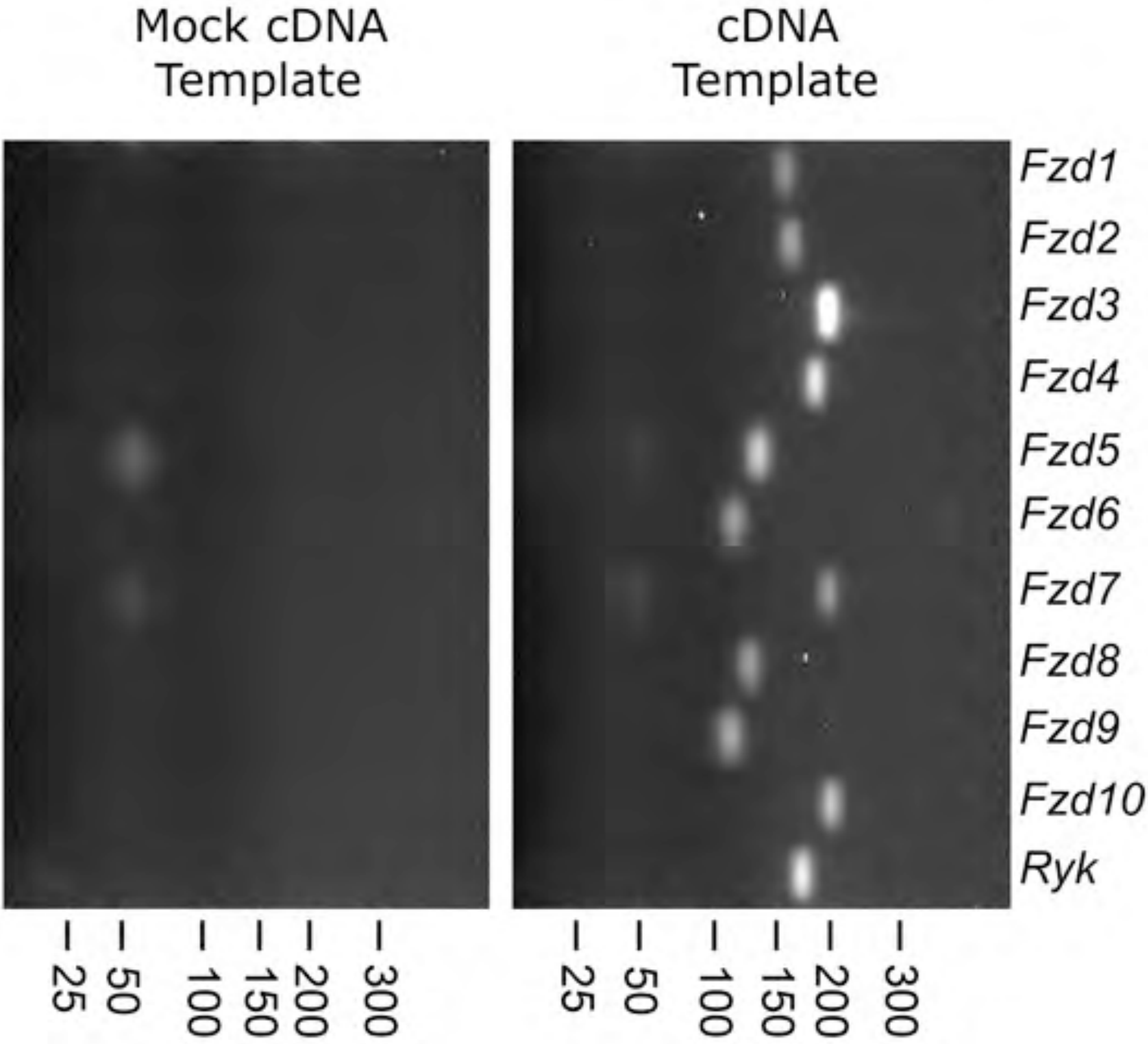
Mock cDNA Template
cDNA Template
Fzd1
Fzd2
Fzd3
Fzd4
Fzd5
Fzd6
Fzd7
Fzd8
Fzd9
Fzd10
Ryk
25
50
100
150
200
300
25
50
100
150
200
300

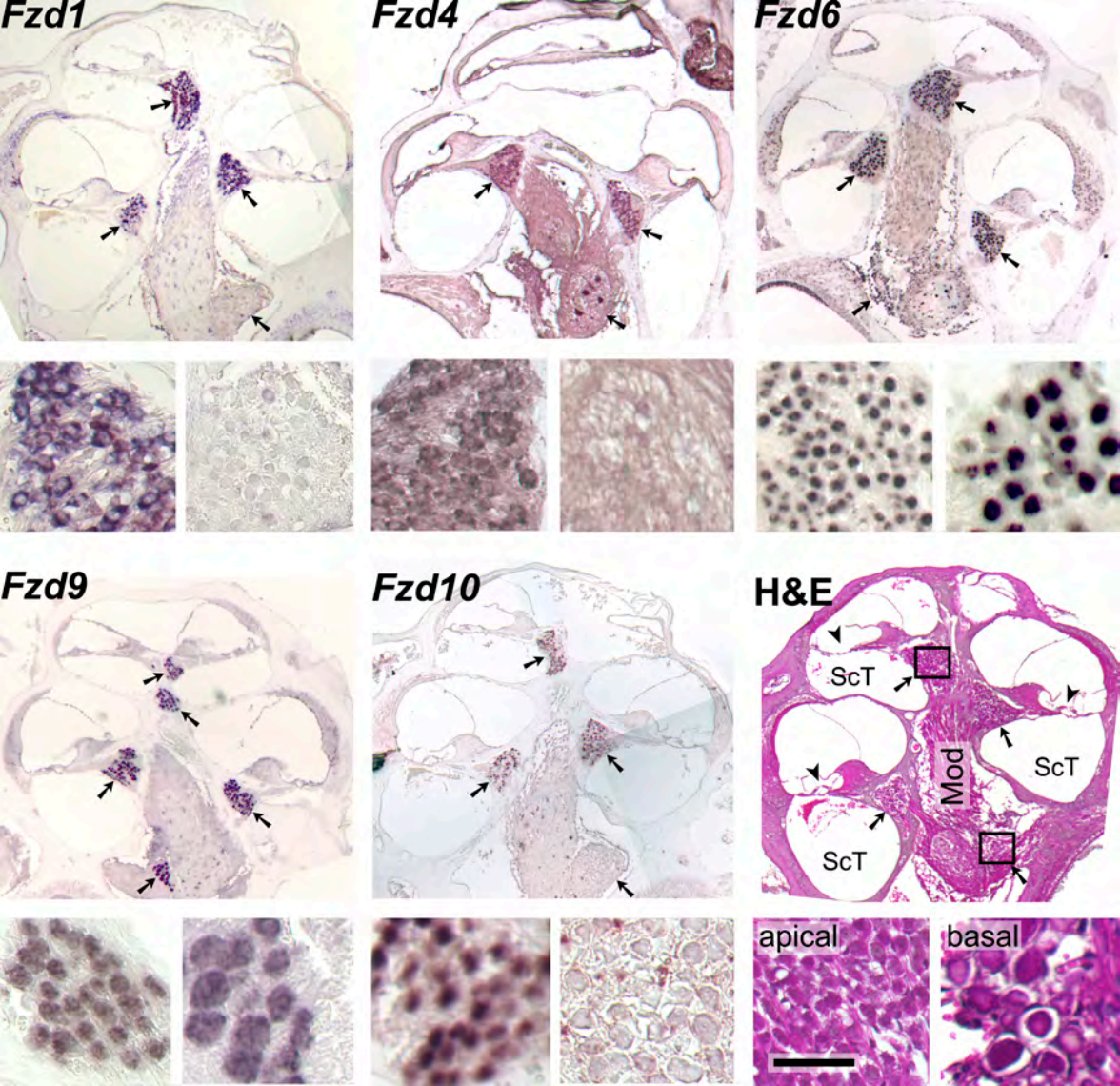
Fzd1
Fzd4
Fzd6
Fzd9
Fzd10
H&E
ScT
Mod
ScT
ScT
apical
basal

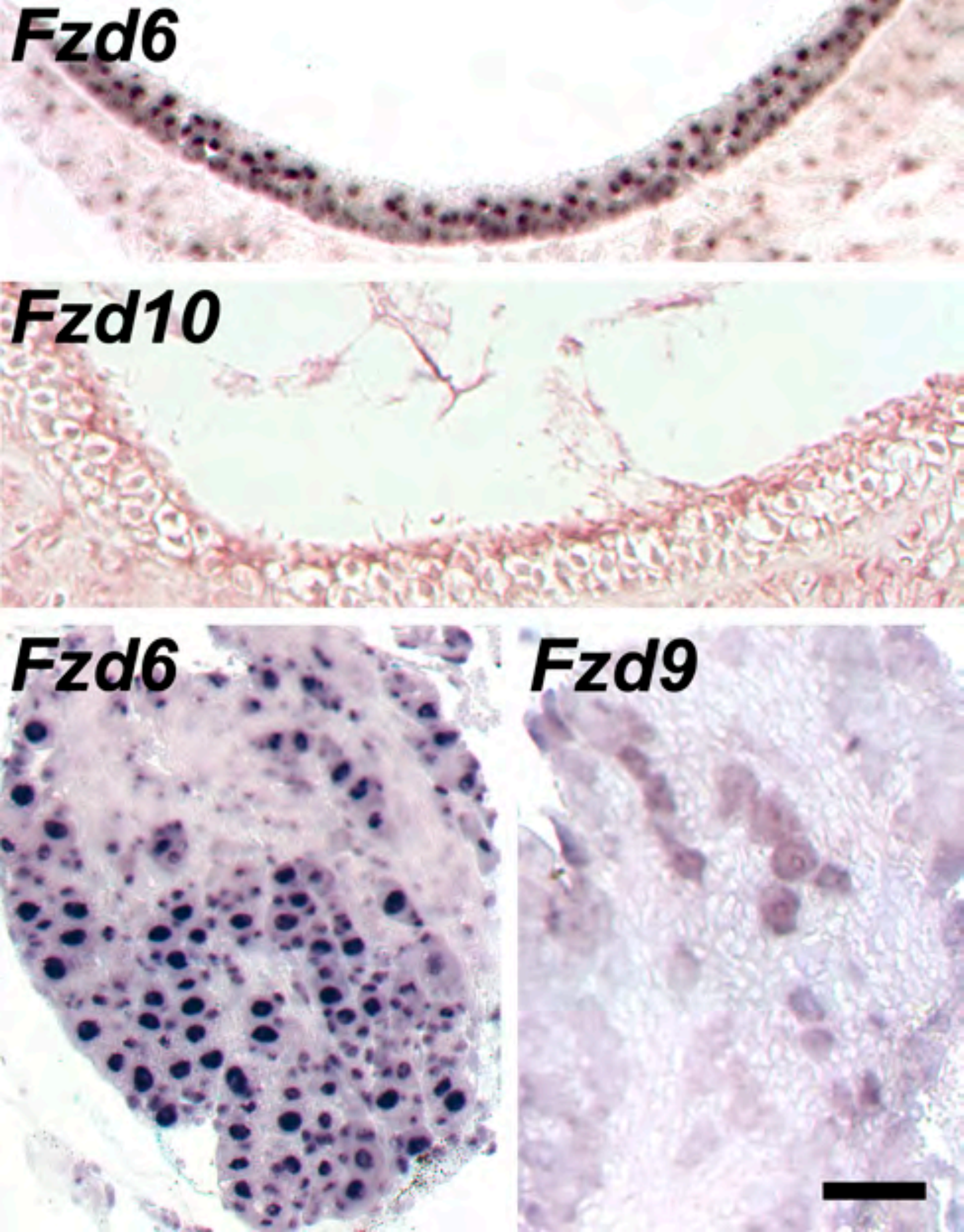
Fzd6
Fzd10
Fzd6
Fzd9

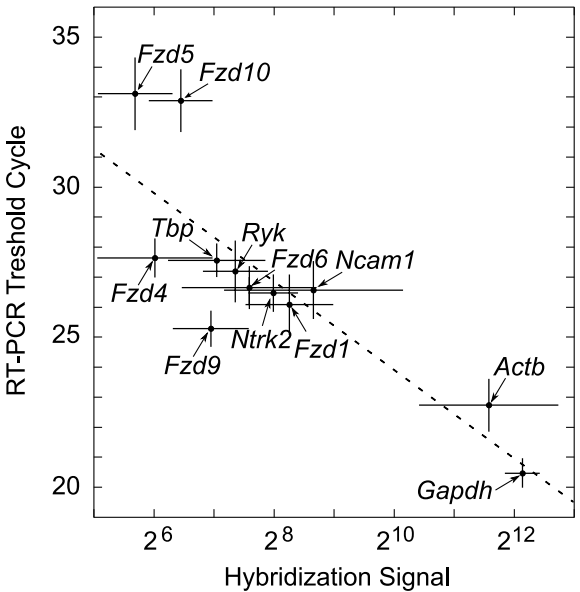
35
30
25
20
RT-PCR Treshold Cycle
Fzd5
Fzd10
Tbp
Ryk
Fzd6
Ncam1
Fzd4
Ntrk2
Fzd1
Fzd9
Actb
Gapdh
2^6
2^8
2^{10}
2^{12}
Hybridization Signal

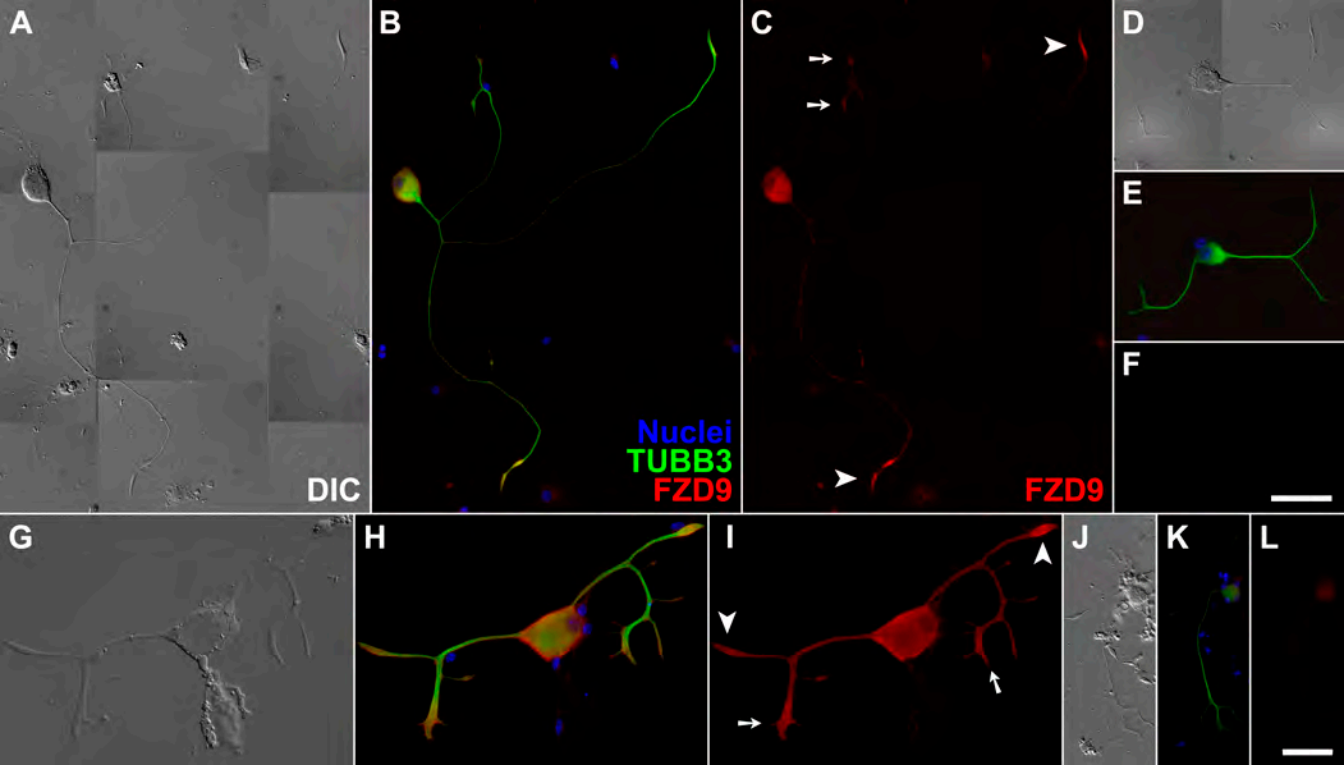
A
DIC
B
Nuclei
TUBB3
FZD9
C
FZD9
D
E
F
G
H
I
J
K
L

Table 1. Oligonucleotide primers

Gene Symbol[a]	Primer Pair (5' to 3')	Product Size (bp)
For qualitative and real-time RT-PCR		
Actb	GGCTGTATTCCCCTCCATCG	154
	CCAGTTGGTAACAATGCCATGT	
Fzd1	GCGACGTACTGAGCGGAGTG	150
	TGATGGTGCGGATGCGGAAG	
Fzd2	CTCAAGGTGCCGTCCTATCTCAG	156
	GCAGCACAACACCGACCATG	
Fzd3	GGTGTCCCGTGGCCTGAAG	194
	ACGTGCAGAAAGGAATAGCCAAG	
Fzd4	GACAACTTTCACGCCGCTCATC	181
	CCAGGCAAACCCAAATTCTCTCAG	
Fzd5	AAGCTGCCTTCGGATGACTA	129
	TGCACAAGTTGCTGAACTCC	
Fzd6	TGTTGGTATCTCTGCGGTCTTCTG	110
	CTCGGCGGCTCTCACTGATG	
Fzd7	ATATCGCCTACAACCAGACCATCC	193
	AAGGAACGGCACGGAGGAATG	
Fzd8	GTTCAGTCATCAAGCAGCAAGGAG	122
	AAGGCAGGCGACAACGACG	
Fzd9	ATGAAGACGGGAGGCACCAATAC	107
	TAGCAGACAATGACGCAGGTGG	
Fzd10	ATCGGCACTTCCTTCATCCTGTC	199
	TCTTCCAGTAGTCCATGTTGAG	
Gapdh	CCCCAATGTGTCCGTCGTG	84
	GCCTGCTTCACCACCTTCT	
Ncam1	CCCAGCCAAGGAGAAATCAG	123
	CTGGTTTGGGCTCAGCTTCT	
Ntrk2	CTGGGGCTTATGCCTGCTG	100
	AGGCTCAGTACACCAAATCCTA	
Ryk	GGTCTTGATGCAGAGCTTTACT	170
	CCCATAGCCACAAAGTTGTCTAC	
Tbp	CCCCACAACTCTTCCATTCT	103
	GCAGGAGTGATAGGGGTCAT	
For cloning partial cDNAs as riboprobe templates		
Fzd1	CAGGTTCTGCAAAAGCTTCC	682
	TCGGTTACTGCACTCCCTCT	
Fzd2	TTTAAAAGCTGCCCTGTGCT	642
	CTACCGGGAGAGAAGGGAAC	
Fzd3	TTTGGGTTGGAAGCAAAAAG	616
	GACACTCTGCCCAAGAAAGC	
Fzd4	AATTCTAGGCAGCCCCTGTT	658
	CCAGCATTCTGGAGGTTCAT	
Fzd5	CACTCAAGACTCCGGAGAGG	607
	TCCTGGGAGTGTAGGTTTGG	
Fzd6	TTGCTAGCCCTGACTGTCCT	613
	CTCCTTTTGGGGAAGGTAGG	
Fzd7	TTTCAAGAGGAGGCCAAGAA	609
	CCCTGTCTGGAGGAAAAACA	
Fzd8	TGGCAGGACATGAGAAAGTG	682
	CGGTTGTGCTGCTCATAGAA	
Fzd9	AGTTTCCTCCTGACCGGTTT	692
	CAAGGCCCTGAGCTTTACTG	
Fzd10	CTTTGCTGCCTGTGCATAAA	616
	CAATAAGCCCTCTGGTGCTC	
Ryk	GAACGACTTGCGAAGTGTCA	700
	CAGAGTCATGAGCTCCCACA	

[a] *Actb*, actin, beta; *Gapdh*, glyceraldehyde-3-phosphate dehydrogenase; *Ncam1*, neural cell adhesion molecule 1; *Ntrk2*, neurotrophic tyrosine kinase, receptor, type 2; *Tbp*, TATA box binding protein.

Table 2. Expression of potential neuronal guidance receptors in the adult cochlea

Gene Symbol[a]	mRNA Level[b]	Other Reports[c]	Gene Symbol	mRNA Level	Other Reports	Gene Symbol	mRNA Level	Other Reports
Ephrin Pathway			*Semaphorin Pathway*			*Netrin Pathway*		
Efna1	5.2±0.4	*i, ii*	*Nrp1*	8.5±1.0 *	*i*	*Dcc*	6.3±0.4 *	*i, vi*
Efna2	5.6±1.3	*i, ii, iii*	*Nrp2*	8.0±0.1 *		*Unc5a*	5.8±0.6	
Efna5	7.5±0.5 *	*i*	*Plxna1*	6.9±0.7 *		*Unc5b*	6.1±1.2	
Efnb1	7.9±0.3 *	*i, iii*	*Plxna2*	7.3±0.4 *		*Unc5c*	7.4±0.4 *	*i*
Efnb2	8.0±1.5 *	*iv, v*	*Plxna3*	5.7±0.7	*i*	*Unc5d*	7.1±1.5 *	
Efnb3	5.8±0.4 *	*v,*	*Plxna4*	5.9±0.4 *		*Wnt Pathway*		
Epha2	6.9±0.4 *		*Plxnb1*	6.0±0.5 *				
Epha4	6.0±2.5	*i, ii, iii*	*Plxnb2*	7.5±1.5 *	*i*	*Fzd1*	8.3±0.7 *	*vii*
Epha5	6.3±0.5 *	*ii*	*Plxnb3*	6.6±1.3		*Fzd2*	7.5±1.2 *	*i, vii*
Epha7	6.6±0.4 *	*i, ii*	*Plxnc1*	7.0±0.8 *		*Fzd3*	5.9±0.7	*vii*
Epha8	5.2±0.7		*Plxnd1*	6.7±0.9 *	*i*	*Fzd4*	6.0±0.9	*i, vii*
Epha10	6.5±0.5 *		*Sema4d*	8.0±0.6 *		*Fzd5*	5.7±0.6	
Ephb1	6.2±0.3 *	*iii, v*	*Sema4f*	6.5±0.7 *		*Fzd6*	7.6±1.1 *	*vii*
Ephb2	6.6±0.9 *	*i, v*	*Sema5a*	7.0±0.9 *		*Fzd7*	7.9±1.1 *	
Ephb3	6.3±0.5 *	*i, iv, v*	*Sema6a*	5.8±0.3 *		*Fzd8*	5.7±0.7	*i*
Ephb4	6.4±0.4 *					*Fzd9*	7.0±0.6 *	*i, vii*
Ephb6	5.6±0.4		*Slit Pathway*			*Fzd10*	6.5±0.5 *	
			Robo1	5.5±2.7		*Lrp6*	5.1±0.2	
			Robo4	5.7±0.4 *	*i*	*Ror1*	5.2±0.5	
						Ryk	7.4±0.5 *	

[a] *Efn…,* ephrins; *Eph…,* Eph receptors; *Nrp…,* neuropilins; *Plxn…,* plexins; *Sema…,* semaphorins; *Robo…,* roundabout homologs; *Dcc…,* deleted in colorectal carcinoma; *Unc…,* unc-5 homologs; *Lrp6,* low density lipoprotein receptor-related protein 6; *Ror…,* receptor tyrosine kinase-like orphan receptor.

[b] Mean ± SD (n = 17) of $\log_2$-transformed and pre-processed microarray hybridization signals in GEO entries GSM321743-8 (modioli of 8-week-old CBA/CaJ mice; this study), GSM108103-8 (4- and 15-month-old C57BL/6 mice; Someya et al., 2007), and GSM109462-6 (9-month-old C57BL/6 mice; Someya et al., 2008).

[c] *i,* CBA/CaJ mice at P32 (Chen and Corey, 2002); *ii,* 2- to 4-month-old mongolian gerbils (Bianchi and Liu, 1999); *iii,* 4- to 34-month-old mongolian gerbils (Bianchi and Gale, 1998); *iv,* adult mice (Bianchi et al., 2002); *v,* adult CD-1 mice (Howard et al., 2003); *vi,* C57 mice at P28 to P35 (Lee and Warchol, 2008); *vii,* Wistar rats at P14 (Daudet et al., 2002).

* Significantly above 44th-percentile cutoff of 5.10 in one-sided t tests with 1,369 probe sets for neuronal transmembrane receptors ($P < 0.05$ after Bonferroni correction).

Supplemental Table 2. Meta-analysis of neuronal transmembrane receptors in our study (GSE12810) and two previous studies by Someya and colleagues (GSE4786 & GSE4866) to estimate absolute expression levels in adult cochlea

For each receptor in the neurotrophic, guidance, and Wnt pathways, the probe set with the strongest hybridization signal is highlighted in green if it exceeded the 44th-percentile cutoff.

Probe Set ID	Gene Symbol	Mean	SD	P_Bonferroni	Pathway
1430014_at	5430419D17Rik	4.50	0.59	1	
1439529_at	A430110N23Rik	6.84	0.84	1.5E-04	
1435584_at	A630033H20Rik	2.97	0.40	1	
1420408_a_at	Abcc9	4.69	0.42	1	
1435751_at	Abcc9	6.68	1.52	0.393	
1435752_s_at	Abcc9	6.87	1.40	0.060	
1448460_at	Acvr1	5.95	0.97	1	
1416787_at	Acvr1	6.12	0.89	0.154	
1416786_at	Acvr1	5.85	0.62	0.084	
1422098_at	Acvr1b	4.84	0.71	1	
1433725_at	Acvr1b	8.15	0.73	6.3E-09	
1443225_at	Acvr1c	3.32	0.33	1	
1428032_at	Acvr1c	4.16	0.47	1	
1438309_at	Acvr1c	4.03	0.67	1	
1457451_at	Acvr2a	3.65	0.91	1	
1437382_at	Acvr2a	8.45	1.28	6.6E-06	
1451004_at	Acvr2a	6.18	0.24	2.3E-09	
1419140_at	Acvr2b	4.95	0.44	1	
1439856_at	Acvr2b	5.32	0.35	1	
1435825_at	Acvrl1	4.46	0.99	1	
1451604_a_at	Acvrl1	5.41	0.51	1	
1439042_at	Adcyap1r1	3.40	0.32	1	
1450799_at	Adcyap1r1	5.91	0.54	9.1E-03	
1429022_at	Adcyap1r1	6.42	0.31	5.1E-09	
1427331_at	Adora1	5.40	0.93	1	
1435495_at	Adora1	6.01	0.39	2.7E-05	
1427519_at	Adora2a	6.15	0.34	5.3E-07	
1460710_at	Adora2a	6.80	0.37	1.4E-09	
1434431_x_at	Adora2b	3.00	0.24	1	
1434430_s_at	Adora2b	2.66	0.18	1	
1450214_at	Adora2b	4.77	0.68	1	
1430482_at	Adora3	2.97	0.30	1	
1429609_at	Adora3	4.23	0.39	1	
1459351_at	Adra1a	3.64	0.56	1	
1421659_at	Adra1a	4.98	0.53	1	
1422183_a_at	Adra1b	5.86	0.37	1.6E-04	
1433601_at	Adra2a	3.53	0.34	1	
1423022_at	Adra2a	4.32	0.49	1	
1433600_at	Adra2a	6.42	0.46	2.0E-06	
1439645_at	Adra2b	4.47	0.42	1	
1450003_at	Adra2b	4.39	0.77	1	
1439762_x_at	Adra2c	3.30	0.23	1	
1457328_at	Adra2c	4.49	0.48	1	
1435296_at	Adra2c	5.93	0.43	4.5E-04	
1422335_at	Adra2c	6.11	0.34	8.0E-07	
1423420_at	Adrb1	3.41	0.16	1	
1437302_at	Adrb2	5.87	0.47	2.9E-03	
1421555_at	Adrb3	4.20	0.33	1	
1455918_at	Adrb3	4.86	1.07	1	
1454003_at	Afg3l2	5.12	0.26	1	
1427206_at	Afg3l2	5.16	0.51	1	
1427207_s_at	Afg3l2	6.69	0.37	3.6E-09	
1436739_at	Agtr1a	4.94	0.87	1	
1446527_at	Agtr1b	4.99	0.43	1	
1415832_at	Agtr2	3.31	0.20	1	
1460596_at	Agtrap	6.17	0.52	1.6E-04	
1422965_at	Agtrap	6.21	0.38	1.2E-06	
1443086_at	Alcam	3.84	0.58	1	
1437466_at	Alcam	8.97	2.78	0.021	
1426301_at	Alcam	8.65	1.25	2.1E-06	
1437467_at	Alcam	8.16	0.98	5.1E-07	
1426300_at	Alcam	7.32	0.69	3.5E-07	
1449987_at	Alk	4.09	0.58	1	
1457021_x_at	Amhr2	4.18	0.29	1	
1427989_at	Amhr2	4.36	0.40	1	
1438967_x_at	Amhr2	4.28	0.67	1	
1425851_a_at	Amigo1	5.02	0.67	1	
1459020_at	Amigo1	5.82	1.42	1	
1447811_s_at	Amigo1	7.38	2.42	0.915	
1427373_at	Amigo1	5.62	0.36	0.014	
1423037_at	Aplnr	5.75	0.53	0.080	
1438651_a_at	Aplnr	6.78	0.59	1.9E-06	
1438373_at	App	3.13	0.25	1	
1438374_x_at	App	3.17	0.46	1	
1420621_a_at	App	8.78	1.31	2.5E-06	
1427442_a_at	App	10.76	0.80	1.7E-12	
1418774_a_at	Atp7a	6.32	0.60	2.1E-04	
1436921_at	Atp7a	7.86	1.24	6.0E-05	
1418603_at	Avpr1a	3.87	0.82	1	
1418604_at	Avpr1a	6.20	0.51	9.9E-05	
1422204_at	Avpr1b	4.53	0.59	1	
1450277_at	Avpr2	5.03	0.60	1	
1438621_x_at	Axl	2.86	0.30	1	
1423586_at	Axl	7.38	0.70	2.9E-07	
1420852_a_at	B3gnt2	4.42	0.96	1	
1450026_a_at	B3gnt2	7.80	1.28	1.3E-04	
1455363_at	Bai1	6.50	0.39	5.9E-08	
1435558_at	Bai2	5.01	0.67	1	
1454782_at	Bai3	5.09	1.07	1	
1424791_a_at	Bcam	6.81	1.33	0.049	
1440770_at	Bcl2	4.80	1.42	1	
1437122_at	Bcl2	6.13	0.80	0.048	
1443837_x_at	Bcl2	5.60	0.38	0.041	
1457687_at	Bcl2	6.89	0.75	2.5E-05	

1422938_at	Bcl2	6.31	0.36	1.4E-07
1450586_at	Bdkrb1	4.02	0.41	1
1442187_at	Bdkrb2	3.42	0.35	1
1422263_at	Bdkrb2	3.37	0.52	1
1445413_at	Bmpr1a	3.38	0.31	1
1425494_s_at	Bmpr1a	6.86	1.07	3.1E-03
1425493_at	Bmpr1a	7.70	1.46	1.2E-03
1425491_at	Bmpr1a	7.13	1.13	1.1E-03
1425492_at	Bmpr1a	8.55	1.12	6.2E-07
1451729_at	Bmpr1a	6.75	0.41	1.1E-08
1443720_s_at	Bmpr1b	2.62	0.18	1
1422872_at	Bmpr1b	4.66	0.40	1
1437312_at	Bmpr1b	4.98	0.57	1
1441652_at	Bmpr2	5.37	0.54	1
1419616_at	Bmpr2	5.75	1.02	1
1434310_at	Bmpr2	10.32	0.90	3.9E-11
1427517_at	Boc	3.12	0.36	1
1426869_at	Boc	7.07	1.36	0.014
1427516_a_at	Boc	7.41	1.44	4.1E-03
1422265_at	Brs3	4.33	0.85	1
1442082_at	C3ar1	4.06	0.33	1
1419482_at	C3ar1	5.15	0.48	1
1419483_at	C3ar1	6.68	0.47	1.5E-07
1422190_at	C5ar1	4.40	0.67	1
1439902_at	C5ar1	5.35	1.04	1
1450510_a_at	Cacna1a	3.17	0.58	1
1444455_at	Cacna1a	4.30	0.44	1
1430408_at	Cacna1a	5.67	0.40	0.017
1459996_at	Cacna1a	6.70	0.73	7.5E-05
1449955_at	Cacna1f	4.78	0.45	1
1418688_at	Calcr	2.95	0.35	1
1418489_a_at	Calcrl	3.91	0.74	1
1459536_at	Calcrl	4.70	0.62	1
1425814_a_at	Calcrl	5.99	2.24	1
1449882_a_at	Casr	4.35	0.67	1
1449881_a_at	Casr	5.13	1.23	1
1422112_at	Ccbp2	3.80	0.76	1
1422111_at	Ccbp2	4.65	0.40	1
1437937_at	Ccbp2	4.89	0.78	1
1421195_at	Cckar	5.19	0.67	1
1460663_at	Cckbr	4.81	0.39	1
1454770_at	Cckbr	4.70	1.29	1
1419610_at	Ccr1	2.93	0.47	1
1419609_at	Ccr1	4.54	0.79	1
1421420_at	Ccr10	4.40	0.43	1
1422349_at	Ccr1l1	3.99	0.61	1
1421187_at	Ccr2	4.26	0.46	1
1421188_at	Ccr2	4.22	1.15	1
1421186_at	Ccr2	4.70	0.53	1
1460067_at	Ccr2	6.15	1.39	1
1422957_at	Ccr3	4.02	0.61	1
1421655_a_at	Ccr4	3.46	0.49	1
1422260_x_at	Ccr5	3.10	0.32	1
1422259_a_at	Ccr5	3.41	0.35	1
1424727_at	Ccr5	4.73	0.65	1
1450357_a_at	Ccr6	4.35	0.51	1
1423466_at	Ccr7	3.52	0.39	1
1422291_at	Ccr8	3.98	0.52	1
1427419_x_at	Ccr9	4.00	0.32	1
1421919_a_at	Ccr9	4.20	0.61	1
1421920_a_at	Ccr9	4.52	0.93	1
1446038_at	Ccr9	4.83	0.62	1
1426139_a_at	Ccrl1	4.18	0.69	1
1437668_at	Ccrl1	5.57	2.08	1
1437669_x_at	Ccrl1	5.54	1.46	1
1427736_a_at	Ccrl2	4.63	0.98	1
1419144_at	Cd163	5.31	0.86	1
1420716_at	Cd247	4.49	0.14	1
1452539_a_at	Cd247	3.61	0.49	1
1426079_at	Cd247	4.45	0.53	1
1426396_at	Cd247	4.96	0.42	1
1452389_at	Cd27	2.84	0.16	1
1422828_at	Cd3d	4.68	0.60	1
1422105_at	Cd3e	6.50	0.62	5.0E-05
1419178_at	Cd3g	3.28	0.40	1
1460415_a_at	Cd40	4.37	0.50	1
1439221_s_at	Cd40	4.62	0.56	1
1449473_s_at	Cd40	5.37	0.54	1
1418353_at	Cd5	3.83	0.61	1
1449193_at	Cd5l	4.87	0.95	1
1451910_a_at	Cd6	5.24	0.74	1
1418830_at	Cd79a	4.93	0.56	1
1417640_at	Cd79b	4.80	0.72	1
1418394_a_at	Cd97	7.61	0.68	4.2E-08
1449637_at	Cdh4	3.47	0.26	1
1449422_at	Cdh4	3.99	0.33	1
1456397_at	Cdh4	6.65	0.32	6.1E-10
1421123_at	Cdk5r1	3.83	0.55	1
1421124_at	Cdk5r1	4.96	0.58	1
1433450_at	Cdk5r1	7.00	1.22	6.0E-03
1433451_at	Cdk5r1	7.38	0.57	1.3E-08
1418925_at	Celsr1	5.40	0.63	1
1422073_a_at	Celsr2	5.93	1.26	1
1435336_at	Celsr2	8.10	1.70	1.3E-03
1425067_at	Celsr3	6.90	1.88	0.776
1418724_at	Cfi	5.23	0.89	1
1417795_at	Chl1	3.31	0.25	1
1443713_at	Chl1	2.92	0.57	1
1447036_at	Chl1	5.24	1.24	1
1435190_at	Chl1	7.11	0.83	2.1E-05
1439611_at	Chrm1	5.74	1.27	1
1450833_at	Chrm1	5.78	0.72	0.903
1422258_at	Chrm3	3.87	0.38	1

1450575_at	Chrm4	4.10	0.39	1	
1444368_at	Chrna3	3.33	0.47	1	
1455931_at	Chrna3	4.22	0.76	1	
1452010_at	Chrna3	5.79	0.68	0.498	
1441837_at	Chrnb2	4.51	0.45	1	
1420744_at	Chrnb2	5.07	0.63	1	
1436428_at	Chrnb2	6.74	0.16	7.2E-15	
1421182_at	Clec1b	5.67	1.24	1	
1419477_at	Clec2d	6.35	0.65	4.9E-04	
1424673_at	Clec2h	2.69	0.17	1	
1431240_at	Clec2h	3.78	0.38	1	
1451438_s_at	Clec2h	4.43	0.55	1	
1422166_at	Clec2i	4.26	0.38	1	
1426072_at	Cmklr1	3.32	0.25	1	
1456887_at	Cmklr1	4.56	0.53	1	
1418980_a_at	Cnp	9.57	1.65	3.9E-06	
1449296_a_at	Cnp	7.38	0.83	3.0E-06	
1437341_x_at	Cnp	10.93	0.82	1.8E-12	
1419425_at	Cnr1	4.89	0.64	1	
1434172_at	Cnr1	5.80	1.44	1	
1450476_at	Cnr2	3.57	0.27	1	
1431663_a_at	Cntfr	4.83	0.42	1	Ciliary neurotrophic factor
1419429_at	Cntfr	7.27	0.21	4.2E-15	Ciliary neurotrophic factor
1419017_at	Corin	3.70	0.37	1	
1425289_a_at	Cr2	4.55	0.63	1	
1418249_at	Crcp	7.41	0.36	1.0E-11	
1427782_a_at	Crhr1	6.61	1.23	0.082	
1418810_at	Crhr1	6.74	0.84	3.8E-04	
1422012_at	Crhr2	3.82	0.41	1	
1450462_at	Crhr2	4.72	0.55	1	
1418097_a_at	Crlf2	5.99	0.63	0.019	
1423593_a_at	Csf1r	6.50	0.83	2.3E-03	
1419872_at	Csf1r	9.28	1.27	2.4E-07	
1419873_s_at	Csf1r	7.74	0.78	1.5E-07	
1420703_at	Csf2ra	4.89	0.43	1	
1421326_at	Csf2rb	5.03	0.56	1	
1455660_at	Csf2rb	5.11	0.93	1	
1450200_s_at	Csf2rb	7.79	0.88	6.4E-07	
1449360_at	Csf2rb2	4.23	0.79	1	
1418806_at	Csf3r	5.37	1.09	1	
1450019_at	Cx3cr1	3.86	0.40	1	
1450020_at	Cx3cr1	5.71	0.29	1.3E-04	
1449195_s_at	Cxcl16	5.67	0.47	0.084	
1418718_at	Cxcl16	7.35	0.52	4.3E-09	
1449925_at	Cxcr3	5.12	0.52	1	
1448710_at	Cxcr4	6.91	1.70	0.309	
1422003_at	Cxcr5	3.19	0.36	1	
1422812_at	Cxcr6	2.60	0.15	1	
1425832_a_at	Cxcr6	3.88	0.47	1	
1417625_s_at	Cxcr7	7.72	1.82	0.014	
1418944_at	Cysltr1	4.00	0.44	1	
1449282_at	Cysltr1	5.00	0.81	1	
1421642_a_at	Cysltr2	4.73	0.54	1	
1432273_a_at	Darc	8.50	0.59	4.1E-11	
1441572_at	Dcc	3.71	0.36	1	Netrin
1440487_at	Dcc	4.90	2.32	1	Netrin
1422162_at	Dcc	6.28	0.44	4.2E-06	Netrin
1415798_at	Ddr1	4.74	0.50	1	
1439382_x_at	Ddr1	5.33	0.96	1	
1435820_x_at	Ddr1	6.27	1.05	0.194	
1456226_x_at	Ddr1	7.18	1.77	0.121	
1415797_at	Ddr1	6.83	0.76	4.4E-05	
1459990_at	Ddr1	6.48	0.59	3.0E-05	
1438367_x_at	Ddr1	6.43	0.35	2.3E-08	
1437619_x_at	Ddr1	7.27	0.33	5.5E-12	
1422738_at	Ddr2	7.12	1.22	2.6E-03	
1455688_at	Ddr2	8.31	1.42	5.2E-05	
1435132_at	Disp1	4.77	0.74	1	
1434795_at	Disp1	6.07	0.28	9.9E-08	
1418287_a_at	Dmbt1	9.54	4.31	0.416	
1455629_at	Drd1a	4.95	0.83	1	
1456051_at	Drd1a	5.28	1.68	1	
1418950_at	Drd2	4.92	0.86	1	
1422278_at	Drd3	3.15	0.36	1	
1422829_at	Drd4	4.06	0.41	1	
1422830_s_at	Drd4	4.46	0.55	1	
1421117_at	Dst	6.14	1.85	1	
1421276_a_at	Dst	5.87	0.98	1	
1430065_at	Dst	5.98	0.71	0.071	
1450119_at	Dst	5.87	0.57	0.031	
1423626_at	Dst	9.90	1.90	1.1E-05	
1449222_at	Ebi3	4.60	0.54	1	
1451691_at	Ednra	3.55	0.66	1	
1460513_a_at	Ednra	4.19	0.85	1	
1440093_at	Ednra	4.66	0.65	1	
1433525_at	Ednra	7.10	1.50	0.033	
1426314_at	Ednrb	5.97	0.50	1.6E-03	
1423594_a_at	Ednrb	6.47	0.58	2.6E-05	
1437347_at	Ednrb	8.57	1.35	8.1E-06	
1447668_x_at	Efemp2	6.91	1.61	0.184	
1417018_at	Efemp2	7.42	0.66	8.0E-08	
1448510_at	Efna1	4.92	0.38	1	Ephrin
1416895_at	Efna1	5.19	0.35	1	Ephrin
1417521_at	Efna2	4.09	0.35	1	Ephrin
1444606_at	Efna2	5.60	1.25	1	Ephrin
1421784_a_at	Efna4	4.77	0.68	1	Ephrin
1421796_a_at	Efna5	3.85	0.30	1	Ephrin
1436866_at	Efna5	7.46	0.53	2.6E-09	Ephrin
1418285_at	Efnb1	6.79	1.27	0.033	Ephrin
1451591_a_at	Efnb1	6.61	0.33	1.2E-09	Ephrin
1418286_a_at	Efnb1	7.87	0.26	2.3E-15	Ephrin
1449549_at	Efnb2	4.36	0.52	1	Ephrin
1449548_at	Efnb2	5.92	0.53	6.0E-03	Ephrin

1419638_at	Efnb2	8.03	1.47	2.8E-04	Ephrin
1419639_at	Efnb2	7.64	1.14	6.0E-05	Ephrin
1423085_at	Efnb3	5.80	0.44	3.9E-03	Ephrin
1457563_at	Egfr	2.94	0.30	1	
1454313_at	Egfr	4.77	0.37	1	
1451530_at	Egfr	4.97	0.63	1	
1432647_at	Egfr	5.02	0.75	1	
1424932_at	Egfr	6.48	1.30	0.333	
1460420_a_at	Egfr	6.26	0.82	0.017	
1435888_at	Egfr	6.88	0.32	7.3E-11	
1418059_at	Eltd1	6.15	0.38	2.4E-06	
1418058_at	Eltd1	6.91	0.34	1.5E-10	
1451161_a_at	Emr1	6.07	1.13	1	
1451563_at	Emr4	3.59	0.45	1	
1424998_at	Emr4	4.17	0.67	1	
1431162_a_at	Enah	5.52	0.65	1	
1442223_at	Enah	6.70	1.14	0.020	
1421624_a_at	Enah	5.96	0.50	1.7E-03	
1424800_at	Enah	9.13	1.72	3.1E-05	
1424801_at	Enah	8.40	0.59	7.7E-11	
1432400_at	Epha1	3.66	0.28	1	Ephrin
1422917_at	Epha1	3.96	0.28	1	Ephrin
1432399_a_at	Epha1	5.07	0.41	1	Ephrin
1436093_at	Epha10	6.54	0.45	4.0E-07	Ephrin
1421151_a_at	Epha2	6.86	0.44	1.2E-08	Ephrin
1426057_a_at	Epha3	3.70	0.40	1	Ephrin
1425574_at	Epha3	3.88	0.46	1	Ephrin
1425575_at	Epha3	4.02	1.40	1	Ephrin
1455426_at	Epha3	4.72	0.74	1	Ephrin
1456863_at	Epha4	2.88	0.61	1	Ephrin
1439757_s_at	Epha4	4.25	1.43	1	Ephrin
1429021_at	Epha4	6.04	2.51	1	Ephrin
1421929_at	Epha4	5.92	1.14	1	Ephrin
1421928_at	Epha4	5.44	0.38	1	Ephrin
1435286_at	Epha5	5.16	1.26	1	Ephrin
1437920_at	Epha5	5.24	1.71	1	Ephrin
1420557_at	Epha5	5.68	0.58	0.543	Ephrin
1444690_at	Epha5	6.31	0.45	4.4E-06	Ephrin
1421527_at	Epha6	4.11	0.52	1	Ephrin
1427528_a_at	Epha7	4.49	0.47	1	Ephrin
1452380_at	Epha7	4.41	1.00	1	Ephrin
1451991_at	Epha7	4.46	0.95	1	Ephrin
1443485_at	Epha7	6.59	0.43	1.1E-07	Ephrin
1419341_at	Epha8	5.25	0.67	1	Ephrin
1455188_at	Ephb1	6.19	0.33	2.1E-07	Ephrin
1425016_at	Ephb2	4.04	0.32	1	Ephrin
1454022_at	Ephb2	6.60	0.89	2.1E-03	Ephrin
1425015_at	Ephb2	6.47	0.57	2.2E-05	Ephrin
1451550_at	Ephb3	6.30	0.51	2.8E-05	Ephrin
1449845_a_at	Ephb4	6.42	0.45	1.1E-06	Ephrin
1418051_at	Ephb6	5.58	0.41	0.119	Ephrin
1423344_at	Epor	5.89	1.35	1	
1424919_at	Erbb2	6.13	0.38	4.3E-06	
1452482_at	Erbb3	4.23	0.76	1	
1434606_at	Erbb3	8.63	0.98	6.4E-08	
1427783_at	Erbb4	2.81	0.25	1	
1458889_at	Evl	4.62	0.79	1	
1440885_at	Evl	5.53	0.32	0.031	
1434920_a_at	Evl	7.29	0.77	2.1E-06	
1450106_a_at	Evl	6.78	0.38	3.1E-09	
1450852_s_at	F2r	7.29	0.89	1.5E-05	
1437308_s_at	F2r	8.19	0.90	1.2E-07	
1448931_at	F2rl1	5.17	0.55	1	
1445680_x_at	F2rl2	3.88	1.00	1	
1421407_at	F2rl2	5.43	1.08	1	
1421288_at	F2rl3	3.92	0.38	1	
1460251_at	Fas	5.91	0.20	1.1E-08	
1425925_at	Fcamr	4.30	0.71	1	
1421775_at	Fcer1a	3.11	0.54	1	
1418340_at	Fcer1g	7.97	1.14	1.1E-05	
1417876_at	Fcgr1	4.32	0.34	1	
1436625_at	Fcgr1	4.65	0.81	1	
1448620_at	Fcgr3	6.11	0.37	3.1E-06	
1425216_at	Ffar2	4.62	1.10	1	
1425215_at	Ffar2	4.97	0.66	1	
1425911_a_at	Fgfr1	6.28	1.40	1	Fibroblast Growth Factor
1436551_at	Fgfr1	7.28	1.13	4.1E-04	Fibroblast Growth Factor
1424050_s_at	Fgfr1	8.11	0.63	9.5E-10	Fibroblast Growth Factor
1420847_a_at	Fgfr2	6.02	0.95	0.692	Fibroblast Growth Factor
1443211_at	Fgfr2	5.81	0.42	2.0E-03	Fibroblast Growth Factor
1433489_s_at	Fgfr2	8.82	1.05	7.8E-08	Fibroblast Growth Factor
1425796_a_at	Fgfr3	3.74	0.35	1	Fibroblast Growth Factor
1421841_at	Fgfr3	6.87	0.40	2.8E-09	Fibroblast Growth Factor
1427776_a_at	Fgfr4	3.04	0.15	1	Fibroblast Growth Factor
1427845_at	Fgfr4	4.14	0.39	1	Fibroblast Growth Factor
1418596_at	Fgfr4	4.38	0.75	1	Fibroblast Growth Factor
1427777_x_at	Fgfr4	5.11	0.80	1	Fibroblast Growth Factor
1427846_x_at	Fgfr4	5.24	1.32	1	Fibroblast Growth Factor
1451912_a_at	Fgfrl1	6.84	0.42	6.6E-09	
1440926_at	Flt1	5.26	0.28	1	
1454037_a_at	Flt1	5.66	0.37	0.010	
1419300_at	Flt1	6.17	0.42	8.2E-06	
1451756_at	Flt1	7.77	0.89	9.1E-07	
1419538_at	Flt3	6.99	0.18	2.7E-15	
1421442_at	Flt4	5.56	0.42	0.250	
1450808_at	Fpr1	4.77	0.67	1	
1421661_at	Fpr3	3.63	0.46	1	
1450583_s_at	Fpr3	3.96	0.41	1	
1450810_at	Fshr	4.36	0.88	1	
1422985_at	Fzd1	4.45	0.74	1	Wnt
1437284_at	Fzd1	8.26	0.72	3.0E-09	Wnt
1440182_at	Fzd10	4.28	0.88	1	Wnt
1455689_at	Fzd10	6.45	0.52	7.4E-06	Wnt

1418533_s_at	Fzd2	4.82	0.96	1	Wnt
1418532_at	Fzd2	5.40	0.90	1	Wnt
1418534_at	Fzd2	7.48	1.18	2.2E-04	Wnt
1450135_at	Fzd3	5.14	0.56	1	Wnt
1420087_at	Fzd3	5.29	0.88	1	Wnt
1421157_at	Fzd3	5.30	0.44	1	Wnt
1449730_s_at	Fzd3	5.86	0.69	0.240	Wnt
1449416_at	Fzd4	3.26	0.27	1	Wnt
1419301_at	Fzd4	6.02	0.95	0.700	Wnt
1422937_at	Fzd5	5.26	0.27	1	Wnt
1455604_at	Fzd5	5.69	0.61	0.693	Wnt
1448662_at	Fzd6	4.81	0.30	1	Wnt
1458904_at	Fzd6	5.22	0.82	1	Wnt
1417301_at	Fzd6	7.59	1.11	5.3E-05	Wnt
1450043_at	Fzd7	4.41	0.43	1	Wnt
1450044_at	Fzd7	7.94	1.14	1.2E-05	Wnt
1445815_at	Fzd8	4.31	0.41	1	Wnt
1423348_at	Fzd8	5.67	0.66	1	Wnt
1427529_at	Fzd9	6.95	0.62	9.7E-07	Wnt
1425595_at	Gabbr1	5.08	0.73	1	
1422051_a_at	Gabbr1	5.16	0.59	1	
1437188_at	Gabbr1	7.75	1.15	3.9E-05	
1455021_at	Gabbr1	9.65	1.30	9.5E-08	
1421281_at	Gabra1	5.48	1.33	1	
1436889_at	Gabra1	5.86	1.86	1	
1421280_at	Gabra1	5.61	1.24	1	
1455766_at	Gabra1	5.87	1.55	1	
1420299_at	Gabra2	2.96	0.19	1	
1421738_at	Gabra2	3.98	0.29	1	
1443865_at	Gabra2	4.83	0.45	1	
1455444_at	Gabra2	4.91	1.49	1	
1421263_at	Gabra3	4.12	0.62	1	
1436957_at	Gabra3	4.78	0.39	1	
1429330_at	Gabra4	4.59	0.44	1	
1433707_at	Gabra4	4.97	0.73	1	
1433602_at	Gabra5	3.92	0.46	1	
1451706_a_at	Gabra6	4.60	1.63	1	
1417121_at	Gabra6	5.32	1.91	1	
1419719_at	Gabrb1	6.40	1.02	0.053	
1450319_at	Gabrb2	4.67	0.91	1	
1429685_at	Gabrb2	5.88	1.11	1	
1428203_at	Gabrb2	5.84	0.88	1	
1428204_at	Gabrb2	6.37	0.94	0.028	
1428205_x_at	Gabrb2	6.25	0.76	8.4E-03	
1421189_at	Gabrb3	4.47	0.40	1	
1421190_at	Gabrb3	4.64	1.30	1	
1435021_at	Gabrb3	6.96	0.78	2.6E-05	
1457763_at	Gabrd	4.11	0.48	1	
1449980_a_at	Gabrd	4.58	1.42	1	
1421629_at	Gabre	5.00	0.51	1	
1427227_at	Gabrg1	3.82	0.48	1	
1460408_at	Gabrg1	4.96	0.58	1	
1437147_at	Gabrg2	4.60	0.49	1	
1418177_at	Gabrg2	6.01	0.94	0.723	
1439717_at	Gabrg3	3.31	0.41	1	
1422187_at	Gabrg3	4.12	0.47	1	
1451424_at	Gabrp	5.39	1.08	1	
1424647_at	Gabrp	6.33	1.21	0.457	
1421536_at	Gabrq	4.55	0.69	1	
1450300_at	Gabrr1	5.51	0.57	1	
1420735_at	Gabrr2	4.82	0.61	1	
1427704_a_at	Galr1	3.32	0.29	1	
1441329_at	Galr1	3.50	0.32	1	
1450568_at	Galr1	4.49	0.64	1	
1422942_at	Galr2	3.64	0.40	1	
1450581_at	Galr3	5.23	0.90	1	
1423537_at	Gap43	5.69	1.42	1	
1456322_at	Gas1	6.08	0.56	1.3E-03	
1448494_at	Gas1	8.23	0.66	8.6E-10	
1416855_at	Gas1	9.39	0.61	1.8E-12	
1450127_a_at	Gcgr	5.63	0.80	1	
1450440_at	Gfra1	4.34	0.89	1	Glial cell line derived neurotrophic factor
1421973_at	Gfra1	5.14	0.73	1	Glial cell line derived neurotrophic factor
1439015_at	Gfra1	7.28	0.48	1.8E-09	Glial cell line derived neurotrophic factor
1425578_a_at	Gfra2	4.59	0.54	1	Glial cell line derived neurotrophic factor
1433716_x_at	Gfra2	4.20	1.01	1	Glial cell line derived neurotrophic factor
1423007_a_at	Gfra2	4.88	0.67	1	Glial cell line derived neurotrophic factor
1425579_at	Gfra2	6.21	1.23	1	Glial cell line derived neurotrophic factor
1459847_x_at	Gfra2	5.59	0.46	0.317	Glial cell line derived neurotrophic factor
1418880_at	Gfra3	6.64	0.85	9.7E-04	Glial cell line derived neurotrophic factor
1450835_a_at	Gfra4	5.78	0.14	3.9E-10	Glial cell line derived neurotrophic factor
1451871_a_at	Ghr	4.85	0.85	1	
1451501_a_at	Ghr	6.02	0.47	2.9E-04	
1417962_s_at	Ghr	8.87	0.82	1.4E-09	
1427611_at	Ghrhr	5.16	0.60	1	
1446756_at	Ghsr	3.71	0.31	1	
1445790_at	Gipr	3.88	0.32	1	
1422330_at	Glp1r	4.70	0.43	1	
1437139_at	Glra1	2.90	0.34	1	
1422277_at	Glra1	3.50	0.57	1	
1434098_at	Glra2	2.83	0.33	1	
1450239_at	Glra3	4.34	0.55	1	
1451937_at	Glra4	3.71	0.66	1	
1427694_at	Gnrhr	3.00	0.23	1	
1427731_at	Gnrhr	3.44	0.60	1	
1421665_a_at	Gnrhr	3.37	0.70	1	
1428250_at	Gper	5.01	0.33	1	
1447583_x_at	Gper	6.35	0.80	5.1E-03	
1460123_at	Gpr1	4.41	0.58	1	
1441382_at	Gpr101	2.76	0.28	1	
1457048_at	Gpr103	2.74	0.26	1	
1419721_at	Gpr109a	4.92	1.11	1	
1421443_at	Gpr110	3.00	0.34	1	

1436230_at	Gpr114	6.04	0.59	4.6E-03
1429460_at	Gpr115	4.19	0.92	1
1457702_at	Gpr12	2.99	0.33	1
1449472_at	Gpr12	4.79	0.93	1
1439489_at	Gpr120	4.06	0.55	1
1418379_s_at	Gpr124	6.37	0.47	4.5E-06
1431034_at	Gpr125	4.07	0.48	1
1444300_at	Gpr125	4.80	0.46	1
1426782_at	Gpr125	6.57	0.78	5.5E-04
1437408_at	Gpr126	6.52	2.02	1
1437409_s_at	Gpr126	6.98	1.13	2.7E-03
1421755_at	Gpr132	3.90	0.48	1
1444233_at	Gpr132	4.30	0.55	1
1455466_at	Gpr133	4.67	0.31	1
1459274_at	Gpr135	4.43	0.61	1
1439346_at	Gpr135	4.65	0.42	1
1441944_s_at	Gpr135	5.78	0.27	1.2E-05
1420581_at	Gpr143	4.49	0.62	1
1443103_at	Gpr146	4.41	0.47	1
1451060_at	Gpr146	4.53	0.46	1
1459864_at	Gpr146	5.65	0.69	1
1423632_at	Gpr146	5.69	0.70	1
1454685_at	Gpr146	7.17	0.24	6.3E-14
1456858_at	Gpr149	3.00	0.27	1
1438210_at	Gpr149	3.20	0.32	1
1431296_at	Gpr15	3.83	0.29	1
1442261_at	Gpr150	2.61	0.21	1
1447485_at	Gpr150	4.82	0.79	1
1457555_at	Gpr151	3.46	0.29	1
1438574_at	Gpr152	5.07	0.47	1
1426973_at	Gpr153	6.48	0.51	4.2E-06
1438526_at	Gpr158	4.77	0.46	1
1459430_at	Gpr158	5.43	0.72	1
1453072_at	Gpr160	4.63	0.78	1
1447353_at	Gpr161	3.55	0.40	1
1418611_at	Gpr162	6.30	1.39	1
1456833_at	Gpr17	4.18	0.31	1
1438439_at	Gpr171	4.88	1.56	1
1429986_at	Gpr173	3.98	0.40	1
1457229_at	Gpr173	5.01	0.42	1
1447792_x_at	Gpr174	2.49	0.15	1
1440900_at	Gpr174	4.43	0.51	1
1442116_at	Gpr176	5.99	0.60	0.010
1439141_at	Gpr18	3.76	0.32	1
1418554_at	Gpr182	5.77	0.26	8.8E-06
1437356_at	Gpr183	4.72	0.51	1
1457691_at	Gpr183	5.39	0.51	1
1445480_at	Gpr19	4.28	0.41	1
1441191_at	Gpr19	4.40	0.65	1
1421756_a_at	Gpr19	6.41	0.46	2.1E-06
1440021_at	Gpr20	5.44	0.80	1
1434673_at	Gpr22	2.98	0.25	1
1434672_at	Gpr22	5.97	0.77	0.174
1440623_at	Gpr26	4.20	0.63	1
1444661_at	Gpr26	5.15	0.67	1
1422154_at	Gpr27	5.11	0.44	1
1460275_at	Gpr3	7.12	0.60	1.5E-07
1451708_at	Gpr33	4.90	0.84	1
1422542_at	Gpr34	4.13	0.60	1
1449976_a_at	Gpr35	4.68	0.59	1
1450875_at	Gpr37	6.16	0.77	0.024
1424146_at	Gpr37l1	7.21	1.15	7.4E-04
1432260_at	Gpr39	6.04	2.44	1
1457745_at	Gpr4	6.11	0.70	0.013
1422275_at	Gpr44	4.86	0.38	1
1450580_at	Gpr45	4.14	0.38	1
1460031_at	Gpr45	5.05	0.99	1
1455498_at	Gpr50	2.91	0.25	1
1450346_at	Gpr50	4.27	0.50	1
1421118_a_at	Gpr56	5.33	0.69	1
1433485_x_at	Gpr56	6.30	0.82	0.013
1440148_at	Gpr6	2.89	0.23	1
1436972_at	Gpr61	5.64	0.30	1.0E-03
1457236_at	Gpr62	3.16	0.29	1
1442138_at	Gpr62	4.26	0.37	1
1422338_at	Gpr63	3.96	0.55	1
1440725_at	Gpr63	4.34	0.52	1
1438350_at	Gpr64	4.36	0.57	1
1439795_at	Gpr64	7.08	1.26	5.0E-03
1449175_at	Gpr65	3.41	0.36	1
1455000_at	Gpr68	6.14	0.28	3.7E-08
1434536_at	Gpr75	5.81	0.95	1
1438411_at	Gpr81	4.58	0.51	1
1439569_at	Gpr83	4.12	0.49	1
1423415_at	Gpr83	5.53	0.75	1
1420591_at	Gpr84	4.30	0.42	1
1459795_at	Gpr85	3.23	0.29	1
1437618_x_at	Gpr85	5.85	0.81	1
1424897_at	Gpr85	6.33	0.99	0.071
1424896_at	Gpr85	5.82	0.51	0.019
1420364_at	Gpr87	4.89	0.49	1
1423171_at	Gpr88	5.39	1.65	1
1460327_at	Gpr88	5.32	0.51	1
1417894_at	Gpr97	4.64	1.06	1
1421693_a_at	Gpr98	3.44	0.58	1
1425314_at	Gpr98	5.06	0.23	1
1437486_at	Gprc5a	5.36	1.30	1
1424613_at	Gprc5b	8.53	1.56	7.3E-05
1451411_at	Gprc5b	7.34	0.92	1.9E-05
1452947_at	Gprc5c	5.44	0.60	1
1424450_at	Gprc5c	5.77	0.61	0.250
1420538_at	Gprc5d	5.34	0.78	1
1428053_at	Gprc6a	4.60	0.70	1

1458285_at	Gria1	4.62	0.50	1
1448972_at	Gria1	5.11	0.58	1
1435239_at	Gria1	6.17	1.33	1
1434146_at	Gria2	6.37	1.94	1
1421970_a_at	Gria2	7.73	1.66	4.7E-03
1453098_at	Gria2	8.21	0.75	7.5E-09
1434728_at	Gria3	6.65	2.77	1
1420563_at	Gria3	5.87	0.90	1
1440891_at	Gria4	4.53	0.71	1
1436772_at	Gria4	5.04	0.82	1
1421351_at	Gria4	5.55	0.38	0.112
1435722_at	Gria4	8.14	1.23	1.5E-05
1421569_at	Grid1	4.55	0.57	1
1441499_at	Grid1	5.48	0.31	0.075
1437824_at	Grid2	2.74	0.15	1
1459245_s_at	Grid2	3.62	0.34	1
1421435_at	Grid2	5.34	0.60	1
1435487_at	Grid2	5.59	1.13	1
1421436_at	Grid2	6.14	0.85	0.080
1439987_at	Grik1	3.95	0.76	1
1427676_a_at	Grik1	5.44	0.54	1
1425790_a_at	Grik2	4.63	0.36	1
1457683_at	Grik2	4.55	0.90	1
1439286_at	Grik2	5.11	0.37	1
1440177_at	Grik3	3.98	0.98	1
1427709_at	Grik3	5.54	0.58	1
1437681_at	Grik4	6.00	0.35	9.1E-06
1418784_at	Grik5	5.76	0.61	0.281
1450202_at	Grin1	5.40	0.36	1
1437968_at	Grin1	7.77	0.60	2.3E-09
1421616_at	Grin2a	3.94	0.58	1
1422223_at	Grin2b	4.32	0.54	1
1457003_at	Grin2b	4.43	0.50	1
1431700_at	Grin2b	5.15	0.76	1
1449245_at	Grin2c	5.04	1.25	1
1421393_at	Grin2d	4.24	0.37	1
1442328_at	Grin2d	6.28	0.35	1.7E-07
1438866_at	Grin3a	3.30	0.29	1
1458378_at	Grin3a	3.83	0.67	1
1436575_at	Grin3a	5.32	0.63	1
1449899_at	Grin3b	5.29	0.41	1
1425700_at	Grm1	4.83	0.71	1
1431344_at	Grm2	4.81	0.78	1
1435607_at	Grm2	5.19	0.92	1
1430136_at	Grm3	5.13	0.60	1
1457299_at	Grm4	7.21	1.03	1.8E-04
1455272_at	Grm5	3.48	0.52	1
1456119_at	Grm5	4.09	0.73	1
1459532_at	Grm7	2.85	0.18	1
1443119_at	Grm7	7.67	2.23	0.151
1421530_a_at	Grm8	4.84	0.70	1
1421470_at	Grpr	3.00	0.52	1
1450260_at	Grpr	4.78	0.59	1
1430336_at	Gucy2g	3.41	0.40	1
1436295_at	Hcrtr1	3.56	0.62	1
1444223_at	Hcrtr2	5.16	0.94	1
1430062_at	Hhipl1	5.32	0.59	1
1420712_a_at	Hpn	4.71	0.36	1
1419210_at	Hrh1	4.13	0.25	1
1438494_at	Hrh1	4.74	0.46	1
1423639_at	Hrh2	5.73	0.80	1
1448807_at	Hrh3	5.52	0.59	1
1426099_at	Hrh4	4.53	0.69	1
1450219_at	Htr1a	4.79	0.50	1
1438710_at	Htr1a	5.08	0.61	1
1422288_at	Htr1b	5.79	0.82	1
1440166_x_at	Htr1d	4.46	0.47	1
1422290_at	Htr1d	4.47	0.68	1
1440741_at	Htr1d	5.11	0.38	1
1440422_at	Htr1f	3.07	0.33	1
1450548_at	Htr1f	4.53	0.74	1
1422125_at	Htr2b	5.54	0.87	1
1450477_at	Htr2c	3.77	0.37	1
1435513_at	Htr2c	4.86	0.59	1
1421652_at	Htr3b	4.56	0.94	1
1443365_at	Htr4	3.93	0.34	1
1427654_a_at	Htr4	3.44	0.55	1
1443276_at	Htr5a	4.09	0.57	1
1422207_at	Htr5a	4.08	0.73	1
1422196_at	Htr5b	4.82	0.75	1
1421757_at	Htr6	3.87	0.36	1
1422235_at	Htr7	3.56	0.31	1
1435332_at	Htr7	6.33	0.85	0.013
1442222_at	Ifnar1	5.24	0.44	1
1449026_at	Ifnar1	6.85	1.07	3.4E-03
1440169_x_at	Ifnar2	5.47	0.93	1
1427691_a_at	Ifnar2	5.60	0.44	0.159
1451462_a_at	Ifnar2	6.61	0.69	7.6E-05
1452108_at	Igf1r	4.72	0.40	1
1446303_at	Igf1r	5.30	0.86	1
1426565_at	Igf1r	5.94	1.19	1
1428967_at	Igf1r	7.43	1.44	3.7E-03
1452982_at	Igf1r	8.78	1.23	9.4E-07
1440979_at	Igf2r	4.02	0.38	1
1424112_at	Igf2r	6.07	1.02	0.830
1424111_at	Igf2r	7.67	0.70	4.8E-08
1427758_x_at	Igh-6	3.83	0.34	1
1452538_at	Igh-6	3.49	0.46	1
1442544_at	Igh-6	3.97	0.62	1
1447998_at	Igh-6	4.37	0.41	1
1451632_a_at	Igh-6	3.86	0.70	1
1426196_at	Igh-6	4.51	0.39	1
1452535_at	Igh-6	4.59	0.51	1

1427869_at	Igh-6	4.40	0.70	1	
1425385_a_at	Igh-6	4.70	0.55	1	
1427756_x_at	Igh-6	4.87	0.64	1	
1425324_x_at	Igh-6	4.97	0.52	1	
1427870_x_at	Igh-6	5.53	1.89	1	
1425247_a_at	Igh-6	5.42	0.97	1	
1427329_a_at	Igh-6	6.48	1.86	1	
1427351_s_at	Igh-6	7.62	2.71	1	
1443646_at	Igsf10	3.33	0.42	1	
1429959_at	Il10rb	4.52	0.22	1	
1419455_at	Il10rb	7.73	0.65	1.1E-08	
1417505_s_at	Il11ra1	7.90	0.85	2.3E-07	
1419530_at	Il12b	3.71	0.39	1	
1449497_at	Il12b	4.37	0.28	1	
1418166_at	Il12rb1	4.54	0.38	1	
1421623_at	Il12rb2	5.59	0.55	1	
1427164_at	Il13ra1	4.40	0.56	1	
1425625_at	Il13ra1	4.58	1.08	1	
1451775_s_at	Il13ra1	5.27	0.82	1	
1454783_at	Il13ra1	5.64	1.10	1	
1427165_at	Il13ra1	6.81	0.42	8.7E-09	
1420678_a_at	Il17rb	5.36	0.41	1	
1421628_at	Il18r1	4.60	0.56	1	
1421291_at	Il18rap	4.79	0.87	1	
1456545_at	Il18rap	5.42	0.68	1	
1459777_at	Il1r1	2.57	0.18	1	
1448950_at	Il1r1	6.35	0.47	4.5E-06	
1419532_at	Il1r2	4.86	1.15	1	
1449585_at	Il1rap	2.97	0.28	1	
1442614_at	Il1rap	3.84	0.35	1	
1421843_at	Il1rap	4.97	0.89	1	
1439697_at	Il1rap	5.39	0.71	1	
1421844_at	Il1rap	6.59	0.57	6.3E-06	
1453373_at	Il1rapl1	4.53	0.55	1	
1427645_a_at	Il1rapl2	2.88	0.23	1	
1446520_at	Il1rapl2	3.31	0.39	1	
1420462_at	Il1rapl2	4.27	0.48	1	
1422317_a_at	Il1rl1	5.10	0.56	1	
1425145_at	Il1rl1	6.07	1.19	1	
1450273_at	Il1rl2	4.41	0.53	1	
1434903_s_at	Il1rl2	4.88	0.32	1	
1450456_at	Il21r	5.03	0.37	1	
1449508_at	Il27ra	5.61	0.53	0.682	
1460598_at	Il28ra	5.66	0.57	0.694	
1420692_at	Il2ra	4.30	0.27	1	
1420691_at	Il2ra	4.68	0.51	1	
1448759_at	Il2rb	4.19	0.63	1	
1417546_at	Il2rb	4.51	0.98	1	
1416295_a_at	Il2rg	4.40	0.98	1	
1416296_at	Il2rg	5.61	1.07	1	
1451535_at	Il31ra	5.87	0.44	1.6E-03	
1419712_at	Il3ra	4.90	0.22	1	
1447858_x_at	Il4ra	4.78	0.69	1	
1421034_a_at	Il4ra	5.04	0.84	1	
1423996_a_at	Il4ra	5.75	0.88	1	
1421620_at	Il5ra	5.04	0.57	1	
1422270_a_at	Il6ra	5.68	0.72	1	
1452416_at	Il6ra	5.78	0.61	0.189	
1421239_at	Il6st	4.65	0.51	1	Ciliary neurotrophic factor & Leukemia inhibitory factor
1437303_at	Il6st	8.06	1.34	7.0E-05	Ciliary neurotrophic factor & Leukemia inhibitory factor
1460295_s_at	Il6st	6.76	0.71	3.3E-05	Ciliary neurotrophic factor & Leukemia inhibitory factor
1452843_at	Il6st	9.20	1.06	2.1E-08	Ciliary neurotrophic factor & Leukemia inhibitory factor
1448576_at	Il7r	3.87	0.46	1	
1448575_at	Il7r	4.41	0.66	1	
1421734_at	Il8rb	5.47	1.30	1	
1421570_at	Il9r	3.93	0.34	1	
1421380_at	Insr	4.32	0.50	1	
1450225_at	Insr	4.46	1.18	1	
1434446_at	Insr	8.14	0.55	8.2E-11	
1420564_at	Insrr	5.87	0.75	0.433	
1427383_at	Irx6	4.10	0.53	1	
1449379_at	Kdr	7.08	0.53	3.1E-08	
1450493_at	Kiss1r	6.39	0.59	8.4E-05	
1415900_a_at	Kit	5.17	0.66	1	
1452514_a_at	Kit	6.48	0.74	6.8E-04	
1458642_at	Klre1	4.32	0.42	1	
1450495_a_at	Klrk1	5.05	1.33	1	
1421958_at	L1cam	4.13	0.48	1	
1450435_at	L1cam	8.35	0.54	2.3E-11	
1449911_at	Lag3	4.54	0.20	1	
1431947_at	Ldlr	4.50	0.44	1	
1459403_at	Ldlr	4.91	0.34	1	
1450383_at	Ldlr	5.39	0.82	1	
1421821_at	Ldlr	8.57	1.49	3.3E-05	
1425873_a_at	Lepr	4.73	0.82	1	
1425644_at	Lepr	4.80	0.90	1	
1425875_a_at	Lepr	5.09	0.69	1	
1456156_at	Lepr	5.28	1.42	1	
1448380_at	Lgals3bp	6.96	1.51	0.076	
1433891_at	Lgr4	8.26	0.70	1.9E-09	
1444519_at	Lgr5	4.80	0.67	1	
1450988_at	Lgr5	5.79	0.57	0.092	
1427028_at	Lgr6	5.14	1.14	1	
1450192_at	Lhcgr	3.53	0.26	1	
1450207_at	Lifr	4.71	0.87	1	
1425107_a_at	Lifr	4.98	0.32	1	Leukemia inhibitory factor
1454984_at	Lifr	9.77	1.23	2.9E-08	Leukemia inhibitory factor
1456234_at	Limk1	4.92	0.89	1	
1417627_a_at	Limk1	8.46	2.55	0.038	
1425836_a_at	Limk1	6.18	0.60	9.9E-04	
1455018_at	Lmtk2	8.38	1.11	1.2E-06	
1452436_at	Loxl2	3.11	0.20	1	
1418269_at	Loxl3	5.51	0.62	1	

1450134_at	Loxl4	3.91	0.49	1	
1421153_at	Loxl4	5.21	0.37	1	
1426110_a_at	Lpar1	5.07	0.57	1	
1417143_at	Lpar1	8.11	1.93	5.5E-03	
1448606_at	Lpar1	9.35	1.37	5.7E-07	
1442291_at	Lpar2	3.69	0.23	1	
1420576_at	Lpar2	4.81	0.60	1	
1418723_at	Lpar3	3.83	0.71	1	
1452424_at	Lpar4	3.84	0.44	1	
1439665_at	Lpar4	3.30	0.72	1	
1434186_at	Lpar4	3.32	1.53	1	
1452812_at	Lphn1	6.74	1.51	0.257	
1428510_at	Lphn1	8.26	0.78	9.8E-09	
1452819_at	Lphn3	4.77	0.37	1	
1458742_at	Lphn3	6.41	1.65	1	
1428523_at	Lphn3	6.06	1.07	1	
1460440_at	Lphn3	7.60	1.64	7.3E-03	
1447551_x_at	Lphn3	7.02	1.07	1.0E-03	
1439313_at	Lphn3	6.36	0.45	2.7E-06	
1416836_at	Lrp10	8.21	0.91	1.3E-07	
1443131_at	Lrp1b	2.73	0.44	1	
1450211_at	Lrp1b	3.85	0.74	1	
1457235_at	Lrp1b	4.06	0.66	1	
1451022_at	Lrp6	5.12	0.22	1	Wnt
1421459_a_at	Lrp8	4.60	0.56	1	
1442347_at	Lrp8	5.40	1.25	1	
1440882_at	Lrp8	5.71	0.64	0.855	
1437825_at	Lrrc4c	5.48	1.02	1	
1437201_at	Lrrc4c	6.36	0.74	1.9E-03	
1447690_at	Lsr	4.70	0.58	1	
1451255_at	Lsr	6.63	0.72	1.3E-04	
1420407_at	Ltb4r1	4.83	0.68	1	
1450807_at	Ltb4r2	3.86	0.75	1	
1460300_a_at	Ltk	5.29	0.54	1	
1453128_at	Lyve1	4.67	0.29	1	
1429379_at	Lyve1	4.57	0.57	1	
1436676_at	Mapk8ip3	3.80	0.94	1	
1416437_a_at	Mapk8ip3	6.34	0.84	0.012	
1425975_a_at	Mapk8ip3	7.07	0.89	6.6E-05	
1449498_at	Marco	3.49	0.38	1	
1458297_s_at	Marco	4.50	0.93	1	
1422936_at	Mas1	3.12	0.38	1	
1422069_at	Mc1r	4.47	0.42	1	
1435393_at	Mc1r	4.68	1.01	1	
1422926_at	Mc2r	4.42	0.74	1	
1422237_at	Mc3r	5.13	0.49	1	
1460723_at	Mc5r	4.80	0.54	1	
1428031_at	Mchr1	3.59	0.30	1	
1454844_at	Mchr1	6.61	1.00	8.2E-03	
1454845_x_at	Mchr1	6.62	0.85	1.1E-03	
1422869_at	Mertk	7.12	0.52	1.9E-08	
1422990_at	Met	4.30	0.57	1	
1434447_at	Met	7.24	0.96	6.1E-05	
1421461_at	Mpl	5.46	1.30	1	
1451919_a_at	Mpl	5.84	0.74	0.541	
1450430_at	Mrc1	7.30	0.76	1.4E-06	
1426141_at	Mrgpra1	3.77	0.34	1	
1451858_at	Mrgpra2	5.40	1.34	1	
1426121_at	Mrgpra3	5.46	1.22	1	
1451926_at	Mrgpra4	3.53	0.33	1	
1437529_at	Mrgprb1	3.23	0.30	1	
1438568_at	Mrgpre	4.64	0.54	1	
1425894_at	Mrgprf	5.77	1.03	1	
1445458_at	Mrgprg	4.88	0.42	1	
1421590_at	Mrgprh	4.48	0.85	1	
1425435_at	Msr1	2.89	0.24	1	
1425434_a_at	Msr1	4.95	0.79	1	
1448061_at	Msr1	5.63	0.53	0.541	
1422062_at	Msr1	5.99	0.84	0.334	
1420461_at	Mst1r	4.42	0.32	1	
1450352_at	Mtnr1a	4.84	0.67	1	
1450511_at	Musk	4.92	0.33	1	
1419272_at	Myd88	6.52	0.97	0.012	
1441057_at	Myh10	3.90	0.35	1	
1452740_at	Myh10	9.05	0.73	1.1E-10	
1440789_at	Neo1	4.11	1.26	1	
1444295_at	Neo1	5.07	1.30	1	
1447694_x_at	Neo1	7.50	0.91	5.6E-06	
1447693_s_at	Neo1	8.26	1.04	7.4E-07	
1434931_at	Neo1	9.05	0.98	1.0E-08	
1423513_at	Neo1	8.05	0.43	3.0E-12	
1456283_at	Neto1	3.26	0.33	1	
1425132_at	Neto1	5.52	1.01	1	
1457344_at	Neto2	4.42	0.40	1	
1454032_at	Neto2	5.10	0.70	1	
1436309_at	Neto2	5.65	0.67	1	
1425714_a_at	Nfam1	3.41	0.52	1	
1428790_at	Nfam1	4.41	0.37	1	
1456068_at	Nfasc	7.82	1.14	2.2E-05	
1459357_at	Nfasc	6.23	0.37	8.5E-07	
1421241_at	Ngfr	4.21	0.53	1	Neurotrophin
1450177_at	Ngfr	4.54	1.07	1	Neurotrophin
1454903_at	Ngfr	8.29	0.84	2.8E-08	Neurotrophin
1422342_at	Nmbr	5.03	0.84	1	
1421667_at	Nmur1	5.55	0.47	0.759	
1425943_at	Nmur2	5.43	0.90	1	
1418633_at	Notch1	6.43	0.36	4.4E-08	
1418634_at	Notch1	7.90	0.49	5.6E-11	
1423086_at	Npc1	7.14	0.59	1.1E-07	
1438514_at	Npc1l1	5.04	0.48	1	
1422214_at	Npffr2	4.23	0.67	1	
1449160_at	Npr1	3.76	0.41	1	
1427191_at	Npr2	8.49	0.81	6.3E-09	

1450286_at	Npr3	4.57	0.34	1	
1448024_at	Npr3	4.83	0.48	1	
1435184_at	Npr3	5.80	1.16	1	
1421471_at	Npy1r	4.72	0.35	1	
1426054_at	Npy1r	4.42	0.64	1	
1417489_at	Npy2r	3.32	0.34	1	
1449312_at	Npy5r	3.65	0.60	1	
1419008_at	Npy5r	4.79	0.85	1	
1438086_at	Npy6r	2.98	0.30	1	
1422347_at	Npy6r	4.58	0.55	1	
1443281_at	Nrcam	4.33	0.51	1	
1458833_at	Nrcam	5.03	0.78	1	
1434709_at	Nrcam	6.56	0.89	3.0E-03	
1430583_at	Nrcam	7.09	0.57	9.1E-08	
1428393_at	Nrn1	9.88	1.49	3.4E-07	
1448944_at	Nrp1	7.84	1.43	4.6E-04	Semaphorin
1448943_at	Nrp1	8.53	1.01	1.5E-07	Semaphorin
1418084_at	Nrp1	7.32	0.47	8.9E-10	Semaphorin
1457198_at	Nrp1	6.82	0.26	5.4E-12	Semaphorin
1447343_at	Nrp2	5.69	0.63	0.951	Semaphorin
1435349_at	Nrp2	7.09	0.82	2.0E-05	Semaphorin
1426528_at	Nrp2	7.97	0.09	1.1E-22	Semaphorin
1426338_a_at	Ntng1	4.41	0.52	1	
1441634_at	Ntng1	5.41	0.74	1	
1449286_at	Ntng1	7.45	1.95	0.096	
1450820_a_at	Ntng2	3.00	0.26	1	
1432033_at	Ntng2	6.20	0.70	5.7E-03	
1443990_at	Ntrk1	4.88	0.84	1	Neurotrophin
1420837_at	Ntrk2	3.98	0.37	1	Neurotrophin
1435305_at	Ntrk2	6.35	1.94	1	Neurotrophin
1446712_at	Ntrk2	5.40	0.45	1	Neurotrophin
1458622_at	Ntrk2	7.40	1.73	0.033	Neurotrophin
1435196_at	Ntrk2	7.22	0.32	5.3E-12	Neurotrophin
1420838_at	Ntrk2	7.99	0.40	1.4E-12	Neurotrophin
1437560_at	Ntrk2	7.67	0.33	4.2E-13	Neurotrophin
1426003_at	Ntrk3	4.37	0.52	1	Neurotrophin
1458707_at	Ntrk3	4.19	0.72	1	Neurotrophin
1425070_at	Ntrk3	4.25	0.93	1	Neurotrophin
1443970_at	Ntrk3	4.82	0.55	1	Neurotrophin
1422329_a_at	Ntrk3	5.21	0.63	1	Neurotrophin
1455917_at	Ntrk3	5.43	1.74	1	Neurotrophin
1425071_s_at	Ntrk3	6.09	1.48	1	Neurotrophin
1433825_at	Ntrk3	7.81	0.88	6.3E-07	Neurotrophin
1420799_at	Ntsr1	3.86	0.71	1	
1417151_a_at	Ntsr2	6.75	0.67	1.5E-05	
1425368_a_at	Numb	4.41	0.94	1	
1416891_at	Numb	7.75	0.68	2.0E-08	
1454098_at	Olfr112	4.38	1.00	1	
1422385_at	Olfr1264	3.61	0.53	1	
1441735_at	Olfr1344	3.03	0.33	1	
1450604_at	Olfr140	4.32	0.79	1	
1422372_at	Olfr15	4.58	0.75	1	
1422371_at	Olfr1507	4.44	0.57	1	
1450600_at	Olfr1508	6.38	0.70	8.4E-04	
1422384_at	Olfr1509	4.05	0.66	1	
1450591_at	Olfr154	4.34	1.06	1	
1422343_at	Olfr155	3.16	0.22	1	
1422337_at	Olfr156	3.32	0.42	1	
1460312_at	Olfr157	3.97	0.71	1	
1450590_at	Olfr159	4.72	0.52	1	
1422382_at	Olfr16	4.44	0.70	1	
1422381_at	Olfr160	5.21	0.65	1	
1422365_at	Olfr17	4.55	0.63	1	
1460313_at	Olfr2	4.47	0.44	1	
1457225_at	Olfr288	4.53	1.07	1	
1445219_at	Olfr315	3.67	0.37	1	
1422351_at	Olfr480	4.05	0.76	1	
1422370_at	Olfr49	3.98	0.54	1	
1422354_at	Olfr544	4.48	0.46	1	
1446400_at	Olfr558	4.81	0.50	1	
1422386_at	Olfr64	6.95	1.47	0.062	
1422363_at	Olfr65	4.33	0.60	1	
1440599_at	Olfr658	3.69	0.24	1	
1450596_at	Olfr66	3.84	0.71	1	
1422374_s_at	Olfr66	4.84	1.03	1	
1450588_at	Olfr67	4.06	0.61	1	
1422360_at	Olfr672	5.20	0.75	1	
1422364_at	Olfr68	4.07	0.67	1	
1450592_at	Olfr69	3.36	0.53	1	
1422362_s_at	Olfr69	5.18	1.05	1	
1422359_at	Olfr690	4.72	0.70	1	
1422367_at	Olfr70	3.71	0.65	1	
1430455_at	Olfr701	4.53	0.71	1	
1432098_a_at	Olfr701	4.80	1.05	1	
1422373_at	Olfr71	4.58	0.43	1	
1421777_at	Olfr73	4.43	0.40	1	
1421776_at	Olfr74	3.59	1.01	1	
1450589_at	Olfr749	4.98	0.88	1	
1421507_at	Olfr78	2.69	0.33	1	
1453535_at	Olfr78	3.64	0.52	1	
1421506_at	Olfr78	4.95	0.80	1	
1440009_at	Olfr78	5.17	0.48	1	
1450597_at	Olfr870	5.14	0.79	1	
1419534_at	Olr1	3.08	0.28	1	
1419723_at	Opn1mw	5.19	0.54	1	
1449132_at	Opn1sw	4.02	0.44	1	
1418552_at	Opn1sw	4.81	0.39	1	
1417677_at	Opn3	5.93	0.70	0.122	
1445121_at	Opn4	3.62	0.30	1	
1421584_at	Opn4	5.15	0.67	1	
1422121_at	Oprd1	3.67	0.60	1	
1446394_at	Oprk1	4.37	0.55	1	
1451813_at	Oprk1	5.58	0.96	1	

1422099_a_at	Oprl1	4.03	0.49	1	
1426204_a_at	Oprl1	4.23	0.69	1	
1450486_a_at	Oprl1	5.35	0.44	1	
1451709_at	Oprm1	3.97	0.45	1	
1451705_a_at	Oprm1	4.06	0.64	1	
1425432_at	Oprm1	4.88	1.07	1	
1459402_at	Oprm1	5.33	1.16	1	
1459217_at	Osmr	4.28	0.46	1	
1418675_at	Osmr	3.95	0.67	1	
1418674_at	Osmr	6.59	0.62	2.1E-05	
1456989_at	Oxgr1	3.70	0.34	1	
1426000_at	Oxtr	4.73	0.48	1	
1440888_at	Oxtr	5.57	0.69	1	
1460719_a_at	P2rx1	4.60	0.58	1	
1429794_a_at	P2rx1	5.24	0.43	1	
1421456_at	P2ry1	4.94	0.37	1	
1452815_at	P2ry10	2.92	0.24	1	
1431724_a_at	P2ry12	5.19	0.65	1	
1428700_at	P2ry13	4.90	0.73	1	
1424733_at	P2ry14	4.77	0.37	1	
1450318_a_at	P2ry2	4.61	0.26	1	
1422276_at	P2ry4	4.23	0.64	1	
1428615_at	P2ry5	7.34	0.34	6.6E-12	
1425214_at	P2ry6	4.83	0.48	1	
1452475_at	Pcsk5	4.17	0.31	1	
1438248_at	Pcsk5	4.10	0.55	1	
1451406_a_at	Pcsk5	4.60	0.47	1	
1424605_at	Pcsk5	4.40	0.74	1	
1437339_s_at	Pcsk5	5.34	0.95	1	
1421916_at	Pdgfra	4.46	0.53	1	
1438946_at	Pdgfra	4.85	0.69	1	
1421917_at	Pdgfra	8.47	1.08	5.1E-07	
1436970_a_at	Pdgfrb	7.51	1.04	3.5E-05	
1417148_at	Pdgfrb	7.48	0.51	1.2E-09	
1450228_a_at	Pip5k1c	6.14	0.76	0.024	
1424954_a_at	Pip5k1c	8.40	0.28	4.8E-16	
1421232_at	Plxna1	4.46	0.31	1	Semaphorin
1428623_at	Plxna1	6.93	0.67	3.3E-06	Semaphorin
1429772_at	Plxna2	4.65	0.40	1	Semaphorin
1451753_at	Plxna2	5.88	0.33	3.1E-05	Semaphorin
1455037_at	Plxna2	6.64	0.55	2.7E-06	Semaphorin
1453286_at	Plxna2	7.28	0.43	3.7E-10	Semaphorin
1420995_at	Plxna3	5.60	0.88	1	Semaphorin
1420996_at	Plxna3	5.71	0.67	1	Semaphorin
1457840_at	Plxna4	4.68	0.55	1	Semaphorin
1441371_at	Plxna4	5.94	0.37	4.9E-05	Semaphorin
1435255_at	Plxnb1	6.54	1.49	0.74	Semaphorin
1435254_at	Plxnb1	6.02	0.52	1.3E-03	Semaphorin
1416683_at	Plxnb2	7.54	1.52	4.1E-03	Semaphorin
1418750_at	Plxnb3	4.66	0.84	1	Semaphorin
1440813_s_at	Plxnb3	6.65	1.23	0.060	Semaphorin
1443433_at	Plxnc1	2.91	0.35	1	Semaphorin
1443434_s_at	Plxnc1	4.15	0.35	1	Semaphorin
1450906_at	Plxnc1	4.08	0.56	1	Semaphorin
1423214_at	Plxnc1	4.25	0.69	1	Semaphorin
1450905_at	Plxnc1	6.09	0.59	2.2E-03	Semaphorin
1423213_at	Plxnc1	7.00	0.78	1.9E-05	Semaphorin
1451475_at	Plxnd1	6.70	0.86	6.5E-04	Semaphorin
1425703_at	Ppard	4.22	0.68	1	
1439797_at	Ppard	5.67	0.81	1	
1422271_at	Ppyr1	4.41	0.83	1	
1451850_at	Prlr	3.64	0.27	1	
1441102_at	Prlr	3.67	0.42	1	
1425853_s_at	Prlr	3.86	0.43	1	
1451844_at	Prlr	4.02	0.59	1	
1450226_at	Prlr	4.30	0.74	1	
1421382_at	Prlr	4.63	0.93	1	
1437397_at	Prlr	5.10	0.45	1	
1448556_at	Prlr	5.33	0.25	1	
1456543_at	Prokr1	3.92	0.52	1	
1450279_at	Prokr1	4.40	0.45	1	
1440564_at	Prokr2	4.35	0.42	1	
1437695_at	Prokr2	4.55	0.41	1	
1420388_at	Prss12	7.09	0.35	5.9E-11	
1421510_at	Prss7	5.01	0.89	1	
1420261_at	Psen1	3.96	0.36	1	
1425549_at	Psen1	4.87	0.48	1	
1450399_at	Psen1	7.82	0.60	1.7E-09	
1421853_at	Psen1	8.43	0.56	2.9E-11	
1427872_at	Ptafr	3.70	0.38	1	
1427871_at	Ptafr	4.45	0.63	1	
1450824_at	Ptch1	4.98	0.78	1	
1439663_at	Ptch1	5.05	0.50	1	
1428853_at	Ptch1	9.11	1.99	2.4E-04	
1422655_at	Ptch2	4.58	0.37	1	
1457256_x_at	Ptch2	8.24	2.45	0.051	
1445703_at	Ptchd1	3.68	0.45	1	
1447996_at	Ptchd1	4.95	0.52	1	
1457649_x_at	Ptchd1	5.67	1.40	1	
1456681_at	Ptchd1	5.31	0.46	1	
1440288_at	Ptchd2	4.94	0.64	1	
1455122_at	Ptchd2	5.77	0.48	0.022	
1431518_at	Ptchd3	5.24	0.38	1	
1422171_at	Ptgdr	5.33	0.33	1	
1450491_at	Ptger1	4.74	0.46	1	
1449310_at	Ptger2	3.80	0.34	1	
1450344_a_at	Ptger3	4.57	0.63	1	
1425251_at	Ptger3	4.84	0.38	1	
1421073_a_at	Ptger4	3.10	0.16	1	
1424208_at	Ptger4	6.74	0.89	6.7E-04	
1449828_at	Ptgfr	3.10	0.20	1	
1446331_at	Ptgfr	3.79	0.41	1	
1440777_x_at	Ptgfr	3.71	0.55	1	

1453924_a_at	Ptgfr	4.54	0.42	1	
1420349_at	Ptgfr	4.73	0.55	1	
1427313_at	Ptgir	5.60	0.55	1	
1452129_at	Pth2r	3.76	0.88	1	
1417092_at	Pthr1	7.25	0.90	2.3E-05	
1430827_a_at	Ptk2	2.77	0.49	1	
1440082_at	Ptk2	4.91	0.37	1	
1443384_at	Ptk2	5.61	0.40	0.060	
1423059_at	Ptk2	6.79	1.13	9.4E-03	
1452589_at	Ptk7	4.82	0.75	1	
1421196_at	Ptpn11	4.92	0.40	1	
1427699_a_at	Ptpn11	5.03	0.34	1	
1451225_at	Ptpn11	9.54	0.71	1.2E-11	
1422589_at	Rab3a	8.72	0.81	2.4E-09	
1459980_x_at	Rab3a	9.89	0.47	5.6E-15	
1437674_at	Rac1	3.61	0.26	1	
1423734_at	Rac1	8.49	0.98	1.1E-07	
1451086_s_at	Rac1	10.55	0.61	4.0E-14	
1421359_at	Ret	5.00	1.04	1	
1436359_at	Ret	6.89	0.89	2.5E-04	Glial cell line derived neurotrophic factor
1443982_at	Rgnef	4.75	0.51	1	
1431161_at	Rgnef	5.43	0.74	1	
1419458_at	Rgnef	5.49	0.39	0.559	
1419457_at	Rgnef	7.04	0.30	7.1E-12	
1422832_at	Rgr	4.01	0.81	1	
1425172_at	Rho	4.37	0.78	1	
1451617_at	Rho	4.17	1.18	1	
1425171_at	Rho	4.93	0.58	1	
1451618_at	Rho	6.24	1.54	1	
1427231_at	Robo1	5.53	2.67	1	Ephrin
1457407_at	Robo1	5.24	0.56	1	Ephrin
1458229_at	Robo2	3.58	0.34	1	Ephrin
1421565_at	Robo3	4.22	0.29	1	Ephrin
1436634_at	Robo3	4.03	0.36	1	Ephrin
1426206_at	Robo4	5.71	0.43	0.02	Ephrin
1429312_s_at	Ror1	3.26	0.39	1	
1451014_at	Ror1	4.51	0.27	1	
1429313_at	Ror1	5.19	0.53	1	Wnt
1423428_at	Ror2	4.04	0.36	1	
1457128_at	Ror2	4.18	0.43	1	
1425970_a_at	Ros1	4.01	0.62	1	
1450280_a_at	Rrh	3.57	0.55	1	
1439650_at	Rtn4	6.20	1.10	0.532	
1437224_at	Rtn4	7.73	1.42	6.9E-04	
1435284_at	Rtn4	7.54	0.83	1.3E-06	
1421116_a_at	Rtn4	8.93	1.02	3.3E-08	
1452649_at	Rtn4	10.60	0.42	1.0E-16	
1419732_at	Rtn4r	5.89	0.51	5.5E-03	
1455664_at	Rtn4rl1	5.14	0.41	1	
1436868_at	Rtn4rl1	6.98	0.76	1.4E-05	
1439573_at	Rtn4rl2	6.98	0.29	7.4E-12	
1440785_at	Rxfp1	3.08	0.24	1	
1440704_at	Rxfp2	3.80	0.38	1	
1421532_at	Rxfp2	4.01	0.56	1	
1447400_at	Ryk	4.76	0.84	1	
1426388_s_at	Ryk	7.13	0.51	1.5E-08	
1451789_a_at	Ryk	7.36	0.53	4.9E-09	Wnt
1423571_at	S1pr1	6.77	0.49	1.5E-07	
1428176_at	S1pr2	4.95	0.23	1	
1447880_x_at	S1pr2	7.23	1.46	0.013	
1460661_at	S1pr3	5.17	1.09	1	
1438658_a_at	S1pr3	7.46	1.06	5.9E-05	
1437173_at	S1pr3	6.83	0.51	1.7E-07	
1451024_at	S1pr4	6.04	0.82	0.146	
1449365_at	S1pr5	4.76	0.53	1	
1431336_at	Scara5	4.35	0.71	1	
1451204_at	Scara5	6.81	1.14	9.1E-03	
1438203_at	Scarf2	4.47	0.36	1	
1438406_at	Scarf2	5.53	0.43	0.612	
1434740_at	Scarf2	6.06	0.65	0.010	
1443454_at	Sctr	4.53	0.55	1	
1425697_at	Sdccag1	4.18	0.27	1	
1429327_at	Sdccag1	4.92	1.21	1	
1429446_at	Sdccag1	8.65	2.13	2.5E-03	
1426455_at	Sdccag10	5.39	1.12	1	
1456106_x_at	Sdccag3	4.69	1.12	1	
1431760_a_at	Sdccag3	5.47	0.35	0.268	
1429554_at	Sdccag3	6.79	0.84	2.4E-04	
1453195_at	Sdccag3	6.37	0.42	8.5E-07	
1453946_a_at	Sdccag8	3.63	0.37	1	
1431203_at	Sdccag8	3.63	0.75	1	
1456538_at	Sdccag8	7.01	1.56	0.079	
1420823_at	Sema4d	4.70	0.76	1	Semaphorin
1420824_at	Sema4d	7.99	0.60	8.4E-10	Semaphorin
1439768_x_at	Sema4f	6.10	0.77	0.043	Semaphorin
1419328_at	Sema4f	6.47	0.73	6.1E-04	Semaphorin
1422167_at	Sema5a	4.15	0.35	1	Semaphorin
1459109_at	Sema5a	3.75	0.66	1	Semaphorin
1434776_at	Sema5a	6.79	1.42	0.103	Semaphorin
1437422_at	Sema5a	7.02	0.94	1.9E-04	Semaphorin
1425903_at	Sema6a	5.01	0.37	1	Semaphorin
1436458_at	Sema6a	6.53	1.26	0.170	Semaphorin
1421414_a_at	Sema6a	5.76	0.26	9.0E-06	Semaphorin
1427571_at	Shh	4.22	0.23	1	
1436869_at	Shh	8.46	0.58	4.3E-11	
1449163_at	Sigirr	5.68	0.71	1	
1451430_at	Slit2	3.49	0.51	1	
1458140_at	Slit2	6.04	1.09	1	
1424659_at	Slit2	8.26	1.14	2.8E-06	
1428089_at	Slitrk1	7.16	0.84	1.6E-05	
1441483_at	Slitrk2	4.97	1.00	1	
1439250_at	Slitrk3	5.45	0.31	0.165	
1437744_at	Slitrk4	4.43	0.46	1	

1429718_at	Slitrk5	5.62	0.24	1.0E-04
1437231_at	Slitrk6	3.66	0.26	1
1442215_at	Smo	3.68	0.96	1
1427048_at	Smo	6.53	2.31	1
1427049_s_at	Smo	6.54	0.75	4.3E-04
1438147_at	Srcrb4d	6.77	0.83	2.4E-04
1450527_at	Sstr1	3.08	0.31	1
1422256_at	Sstr2	4.05	0.71	1
1441603_at	Sstr3	3.66	0.50	1
1450577_at	Sstr3	4.63	0.34	1
1422281_at	Sstr4	4.42	0.38	1
1457440_at	Sstr4	6.78	0.31	8.9E-11
1445459_at	Sstr5	4.90	0.75	1
1457828_at	Stam	4.87	0.55	1
1459427_at	Stam	5.14	0.83	1
1416862_at	Stam	5.47	0.61	1
1416861_at	Stam	6.28	0.70	2.1E-03
1440034_at	Stam2	4.64	0.41	1
1453338_at	Stam2	5.30	0.93	1
1416977_at	Stam2	5.62	0.68	1
1416975_at	Stam2	5.61	0.30	2.5E-03
1416976_at	Stam2	7.39	0.51	2.3E-09
1416974_at	Stam2	7.00	0.33	4.7E-11
1418804_at	Sucnr1	3.47	0.27	1
1422355_at	Taar1	5.24	0.98	1
1422282_at	Tacr1	4.90	0.59	1
1422234_at	Tacr2	4.67	0.66	1
1440803_x_at	Tacr3	3.93	0.59	1
1450278_at	Tacr3	5.22	0.69	1
1437029_at	Tacr3	5.83	1.03	1
1420432_at	Tas1r1	4.22	0.50	1
1450313_at	Tas1r2	6.34	0.82	8.4E-03
1420778_at	Tas1r3	5.46	0.54	1
1422389_at	Tas2r105	3.56	0.63	1
1450605_at	Tas2r108	5.63	1.02	1
1450585_at	Tas2r119	4.15	0.49	1
1419222_at	Tbxa2r	6.41	1.18	0.206
1418788_at	Tek	6.48	0.97	0.017
AFFX-TransRecMur/X57349_5_at	Tfrc	3.31	0.36	1
AFFX-TransRecMur/X57349_M_at	Tfrc	3.73	0.81	1
1422967_a_at	Tfrc	5.09	1.00	1
AFFX-TransRecMur/X57349_3_at	Tfrc	5.40	1.14	1
1422966_a_at	Tfrc	6.46	0.67	2.1E-04
1452661_at	Tfrc	10.28	1.25	7.0E-09
1420894_at	Tgfbr1	4.50	0.59	1
1420893_a_at	Tgfbr1	4.57	0.73	1
1420895_at	Tgfbr1	7.71	0.95	3.3E-06
1448529_at	Thbd	8.40	2.19	8.3E-03
1444373_at	Tiam1	3.89	0.29	1
1453887_a_at	Tiam1	3.44	0.49	1
1418057_at	Tiam1	7.56	1.03	2.3E-05
1416238_at	Tie1	4.88	0.69	1
1418685_at	Tirap	5.18	0.38	1
1457676_at	Tirap	6.89	1.42	0.060
1449049_at	Tlr1	3.96	0.47	1
1438329_at	Tlr12	4.41	0.38	1
1437931_at	Tlr12	5.16	0.50	1
1457753_at	Tlr13	4.82	0.37	1
1419132_at	Tlr2	4.76	0.85	1
1422781_at	Tlr3	4.52	0.89	1
1422782_s_at	Tlr3	7.16	1.87	0.226
1442827_at	Tlr4	3.41	0.23	1
1430695_at	Tlr4	3.87	0.78	1
1418163_at	Tlr4	4.46	0.64	1
1418162_at	Tlr4	5.56	0.93	1
1450242_at	Tlr5	5.42	0.63	1
1421352_at	Tlr6	4.40	0.43	1
1422010_at	Tlr7	4.03	0.49	1
1449640_at	Tlr7	4.63	0.84	1
1419848_x_at	Tlr7	4.76	0.85	1
1450267_at	Tlr8	4.67	1.30	1
1422083_at	Tlr9	4.92	0.46	1
1445244_at	Tm2d1	4.43	0.67	1
1426254_at	Tm2d1	6.54	0.84	1.8E-03
1451996_at	Tm2d1	7.10	0.58	1.1E-07
1427477_at	Tmprss13	5.68	0.65	1
1449369_at	Tmprss2	4.04	0.42	1
1459510_at	Tmprss2	4.72	0.64	1
1419154_at	Tmprss2	5.30	1.17	1
1458347_s_at	Tmprss2	8.21	0.54	4.2E-11
1421714_at	Tmprss3	5.58	0.70	1
1426302_at	Tmprss4	4.54	0.76	1
1418959_at	Tmprss5	6.14	0.94	0.206
1421296_at	Tnfrsf10b	3.85	0.37	1
1422344_s_at	Tnfrsf10b	4.25	0.44	1
1418571_at	Tnfrsf12a	7.32	0.70	4.0E-07
1418572_x_at	Tnfrsf12a	7.17	0.51	8.5E-09
1417291_at	Tnfrsf1a	8.21	1.20	7.1E-06
1448951_at	Tnfrsf1b	4.36	0.78	1
1418099_at	Tnfrsf1b	6.03	0.50	5.9E-04
1420351_at	Tnfrsf4	5.76	1.51	1
1421226_at	Trem2	5.55	0.86	1
1421792_s_at	Trem2	5.46	0.38	0.845
1459994_x_at	Trfr2	4.44	0.84	1
1425381_a_at	Trfr2	6.20	1.18	0.933
1449571_at	Trhr	2.85	0.27	1
1449572_at	Trhr	3.15	0.39	1
1450356_at	Trhr2	6.12	0.73	0.021
1417545_at	Trpv4	5.57	0.66	1
1428001_at	Tshr	3.10	0.26	1
1421999_at	Tshr	4.06	0.48	1
1442300_at	Tshr	5.18	0.87	1
1450041_a_at	Tub	3.72	0.59	1

1420925_at	Tub	6.02	1.10	1	
1451582_at	Tulp1	4.56	0.51	1	
1425249_a_at	Tyro3	5.47	0.83	1	
1425248_a_at	Tyro3	5.75	0.52	0.075	
1416504_at	Ulk1	5.91	0.67	0.093	
1448370_at	Ulk1	7.61	0.35	1.4E-12	
1434095_at	Unc5a	5.80	0.64	0.229	Netrin
1453269_at	Unc5b	4.28	0.54	1	Netrin
1435110_at	Unc5b	6.09	1.17	1	Netrin
1419592_at	Unc5c	4.54	0.50	1	Netrin
1449522_at	Unc5c	7.44	0.38	1.3E-11	Netrin
1440484_at	Unc5d	7.05	1.49	0.04014533	Netrin
1451863_at	Uts2r	4.47	0.94	1	
1450558_at	V1ra1	3.10	0.55	1	
1427675_at	V1ra2	3.20	0.35	1	
1450603_s_at	V1ra3	3.11	0.44	1	
1450598_at	V1ra4	2.92	0.31	1	
1422368_at	V1ra5	3.12	0.39	1	
1422369_at	V1ra6	4.53	1.01	1	
1422366_at	V1ra9	4.81	0.93	1	
1422376_at	V1rb1	3.06	0.19	1	
1422356_at	V1rb10	2.79	0.23	1	
1421778_at	V1rb2	2.92	0.37	1	
1450599_at	V1rb3	3.37	0.52	1	
1422377_at	V1rb4	6.48	1.08	0.051	
1422378_at	V1rb7	2.84	0.28	1	
1450601_at	V1rb8	3.53	0.48	1	
1422379_x_at	V1rb9	3.89	0.33	1	
1451097_at	Vasp	7.87	0.92	8.2E-07	
1423004_at	Vipr1	3.50	0.44	1	
1455555_at	Vipr1	4.21	0.67	1	
1421391_at	Vipr2	4.78	0.63	1	
1421715_at	Vmn2r1	6.56	1.05	0.020	
1420079_at	Vmn2r107	3.46	0.47	1	
1421719_at	Vmn2r26	5.73	1.01	1	
1450331_s_at	Vmn2r42	5.81	1.13	1	
1427686_at	Vmn2r88	2.85	0.30	1	
1427681_s_at	Vmn2r88	3.33	0.50	1	
1422294_at	Xcr1	3.67	0.47	1	